

Stream chemical response is mediated by hydrologic connectivity and fire severity in a Pacific Northwest forest

Sidney A. Bush¹  | Sherri L. Johnson²  | Kevin D. Bladon³  | Pamela L. Sullivan¹ 

¹College of Earth, Ocean, and Atmospheric Science, Oregon State University, Corvallis, Oregon, USA

²U.S. Department of Agriculture, Forest Service, Pacific Northwest Research Station, Corvallis, Oregon, USA

³Department of Forest Ecosystems and Society, College of Forestry, Oregon State University, Corvallis, Oregon, USA

Correspondence

Sidney A. Bush, College of Earth, Ocean, and Atmospheric Science, Oregon State University, Corvallis, OR 97331, USA.

Email: bushsi@oregonstate.edu

Funding information

National Science Foundation, Grant/Award Numbers: EAR-2034232, EAR-2012796; National Science Foundation, Grant/Award Number: DEB-2025755

Abstract

Large-scale wildfires are becoming increasingly common in the wet forests of the Pacific Northwest (USA), with predicted increases in fire prevalence under future climate scenarios. Wildfires can alter streamflow response to precipitation and mobilize water quality constituents, which pose a risk to aquatic ecosystems and downstream drinking water treatment. Research often focuses on the impacts of high-severity wildfires, with stream biogeochemical responses to low- and mixed-severity fires often understudied, particularly during seasonal shifts in hydrologic connectivity between hillslopes and streams. We studied the impacts of the 2020 Holiday Farm Fire at the HJ Andrews Experimental Forest where rare pre-fire stream discharge and chemistry data allowed us to evaluate the influence of mixed-severity fire on stream water quantity and quality. Our research design focused on two well-studied watersheds with low and low-moderate burn severity where we examined long-term data (pre- and post-fire), and instantaneous grab samples collected during four rain events occurring immediately following wildfire and a prolonged dry summer. We analysed the impact of these rain events, which represent the transition from low-to-high hydrologic connectivity of the subsurface to the stream, on stream discharge and chemistry behaviour. Long-term data revealed total annual flows and mean flows remained fairly consistent post-fire, while small increases in baseflow were observed in the low-moderately burned watershed. Stream water concentrations of nitrate, phosphate and sulfate significantly increased following fire, with variance in concentration increasing with fire severity. Our end member mixing models suggested that during rain events, the watershed with low-moderate severity fire had greater streamflow inputs from soil water and groundwater during times of low connectivity compared to the watershed with low severity fire. Finally, differences in fire severity impacts on concentration-discharge relationships of biogenic solutes were most expressed under low catchment connectivity conditions. Our study provides insights into post-wildfire impacts to stream water quality, with the goal of informing future research on stream chemistry responses to low, moderate and mixed severity wildfire.

KEY WORDS

concentration-discharge, end-member mixing, Holiday Farm Fire, hysteresis, mixed-severity fire, Oregon, rain events, wet forests

1 | INTRODUCTION

Warmer temperatures, shifts in precipitation patterns, and increased drought severity have contributed to recent increases in the occurrence of large wildfires in the Pacific Northwest (PNW) of the United States (Westerling, 2016; Reilly et al., 2022; Holden et al., 2018). Wildfire can result in reduced ground cover and loss of overstory and riparian vegetation, which can lead to an influx of sediment, ash, and burned material into waterways (Nyman et al., 2011) and pose a threat to aquatic ecosystem health (Bladon et al., 2014; Emelko et al., 2016; Niemeyer et al., 2020). Rainfall following wildfire in forested catchments can additionally alter stream water quality through the rapid mobilization and transport of burned material from hillslopes to streams (Murphy et al., 2012). Wildfires alter the physical properties of the soil surface in many ways that influence the hydrological response of burned catchments to rain events such as increasing soil-water hydrophobicity, soil sealing, surface crust formation, soil pore clogging, and changes in bulk density (Agbeshie et al., 2022; Balfour et al., 2014; Doerr et al., 2000; Larson-Nash et al., 2018; Nyman et al., 2014). These effects on soil physical properties influence soil hydraulic properties like hydraulic conductivity and sorptivity, which can reduce infiltration or shift runoff generation pathways (Ebel & Moody, 2017). Such changes can increase runoff response, potentially leading to elevated peak flows, low flows, and annual discharge (Bart, 2016; Kinoshita et al., 2014; Lavabre et al., 1993; Wine et al., 2018). Runoff response can be additionally complicated by the spatial heterogeneity of wildfire impacts across a landscape, particularly following mixed severity burns, which results in highly localized impacts to soil hydrologic properties (McGuire et al., 2021). In the PNW, rainfall following wildfire typically occurs after prolonged dry summers that lead to an increased period of hydrologic connectivity in the fall, yet the interaction between these natural shifts in connectivity and the physical and chemical changes of streams following wildfire remain unclear.

Many studies have used end-member mixing analysis (EMMA) to identify runoff contributions to streamflow (Birch et al., 2021; Christophersen & Hooper, 1992; Hooper & Shoemaker, 1986; Kiewiet et al., 2020; Sklash & Farvolden, 1979) and to assess connectivity of uplands to streams (Bush et al., 2023; Tetzlaff et al., 2015; Uhlenbrook et al., 2004). Because stream chemistry is the proportional mixture of all actively contributing sources within a catchment, chemically quantifying each source, or end-member, allows for quantification of hydrologic connectivity between sources within the catchment to the stream. An additional technique for better understanding the relationship between stream chemistry and hydrologic regime involves analysing the relationships between stream chemical solute concentrations and discharge during a given rain event (Godsey et al., 2009; Lloyd et al., 2016). Stream solutes often exhibit a cyclical relationship between concentration and discharge on the event scale, and concentration-discharge (C-Q) relationships can reveal hydrochemical processes and aid in inferring the origin and fate of materials transported (Bowes et al., 2015; Butturini et al., 2008; Evans & Davies, 1998; Lawler et al., 2006). The direction or rotational pattern of the C-Q hysteresis is indicative of increases or decreases in

concentration with discharge. Clockwise hysteresis occurs when greater concentrations are measured on the rising limb of the hydrograph as a result of rapid flushing and exhaustion of material from within or near channel sources (Bieroza & Heathwaite, 2015). In contrast, anticlockwise hysteresis is typically associated with delayed solute delivery from the deeper subsurface sources and greater concentration on the falling limb (Bieroza & Heathwaite, 2015; Gellis, 2013). However, antecedent moisture conditions may complicate our interpretation of hysteretic relationships by influencing the direction and magnitude of hysteresis in solute transport (Ávila et al., 1992; Bieroza & Heathwaite, 2015; Butturini et al., 2006; Guarch-Ribot & Butturini, 2016).

Our study occurred following the 2020 Holiday Farm Fire at HJ Andrews (HJA) Experimental Forest in Oregon, United States. HJA is located in a Mediterranean ecosystem, defined by highly seasonal precipitation with episodic, large amounts of rainfall during cool winters followed by a warm, dry season in the summer (Bonada & Resh, 2013). Such a transition between dry and wet periods greatly alters the hydrologic connectivity between the landscape and stream (Bernal et al., 2013). As overall catchment moisture increases, contributing areas become connected (Jencso et al., 2009; Nippgen et al., 2015; Smith et al., 2013), increasing the proportion of the catchment that is hydrologically connected to the stream (D'Odorico & Rigon, 2003; Jencso et al., 2009; Nippgen et al., 2011, 2015; Smith et al., 2013). Changes in hydrologic connectivity can be further exacerbated by disturbances like wildfire (Ebel & Moody, 2017). Fortunately, four rain events with increasing precipitation totals occurred immediately following the Holiday Farm Fire at the start of the transition from the dry summer to wet winter season in 2020. We used a combination of EMMA and C-Q hysteresis analysis to understand how low to moderate burn severity impacted stream discharge, stream chemistry, and the activation of hydrologic flow paths during this series of rain events that increasingly enhanced catchment hydrologic connectivity. The HJA also has an extensive database that enabled us to compare long-term pre-fire stream chemistry to post-fire stream chemistry.

Here we examined the influence of antecedent moisture conditions during the seasonal fall wet-up and during rain events to answer the following research questions: (1) what is the impact of mixed severity wildfire on streamflow and stream chemistry; (2) how do increases in antecedent moisture conditions following rain events impact stream chemistry; and (3) how might wildfire and increased wetting influence flow paths and routing of water delivery to streams? Our study provides a lens for evaluating post-fire shifts in hydrologic flow paths and source water contributions to streams with implications for water quality delivery to downstream systems.

2 | MATERIALS AND METHODS

2.1 | Study area

Our study was conducted at the HJ Andrews Experimental Forest (HJA; 44.23°N, 122.17°W), a 6400-ha forested catchment containing

Lookout Creek in the Western Cascades, Oregon, USA (Figure 1). HJA has been a long-term study site for ecological and forest management research for more than 70 years. Elevation across the catchment ranges between approximately 410 and 1630 m. The climate is characterized as Mediterranean, with mild, wet winters, and warm, dry summers. Mean annual air temperature is 8.5°C, ranging from 0.6°C in December to 17.8°C in July. Mean annual precipitation ranges from 2200 mm to >3300 mm, with greater accumulation at upper elevations, and more than 80% of annual precipitation falling between

November and June (Jones & Perkins, 2010). The HJA spans the rain-to-snow transition zone; snow rarely persists for more than a few weeks at low elevation, but above 1000 m, seasonal snowpack can persist through the winter or accumulate and melt several times (Bierlmaier & McKee, 1989; Johnson et al., 2021; Jones & Perkins, 2010). HJA contains multiple small experimental watersheds that are gaged and routinely sampled. Three of the lower elevation watersheds were impacted by the Holiday Farm Fire in 2020 (Figure 1; Watersheds 1, 2 and 9).

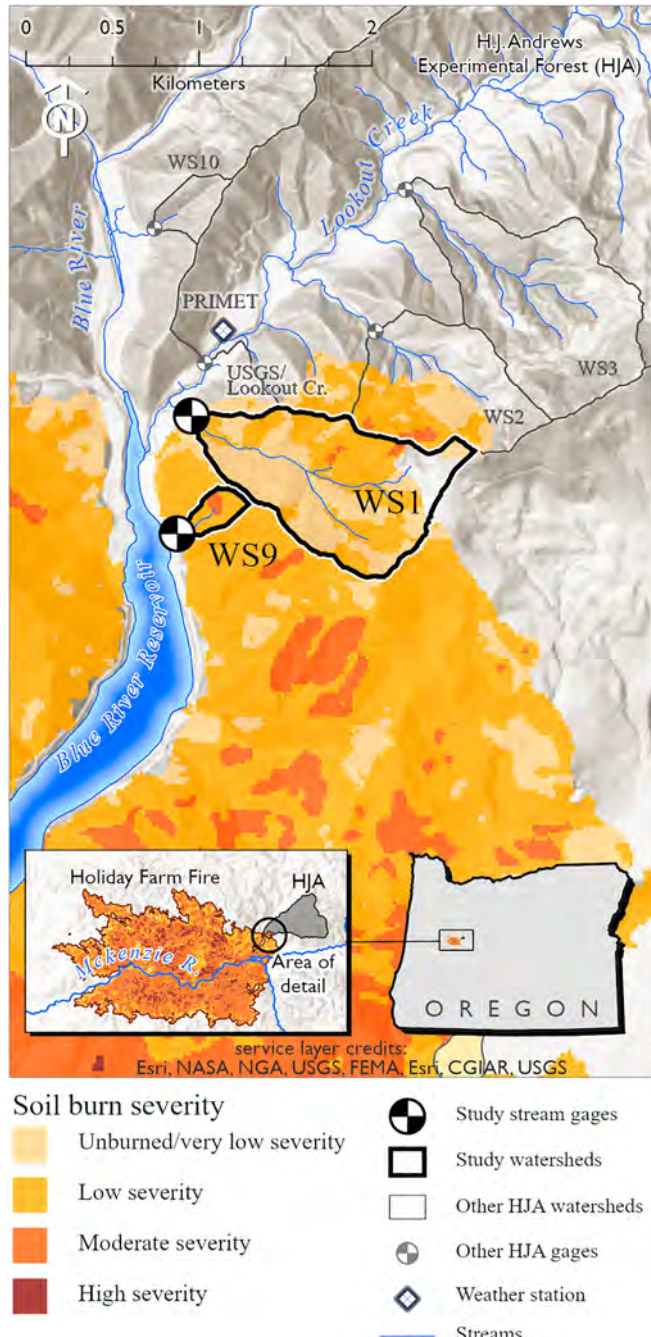


FIGURE 1 Map of the location and burn severity of the Holiday Farm Fire and impacted experimental watersheds within the H.J. Andrews Experimental Forest.

2.1.1 | The Holiday Farm Fire

The Holiday Farm Fire ignited the night of 7 September 2020, and burned roughly 70 188 ha of the McKenzie River Watershed, making it one of the largest forest fires in Oregon's history. Fire entered HJA on September 12th at the south boundary of Watershed 9 (WS9), and gradually progressed northward into Watershed 1 (WS1), and Watershed 2 (WS2) (Figure 1). Soil burn severity was higher across the full area of the Holiday Farm compared to that of the HJA experimental watersheds, with a lower percentage of low severity burn (24%) and a higher percentage of moderate and high severity burn (62% and 9%, respectively) (Table 1) (USDA Forest Service, 2020). While a greater proportion of WS1 burned at high severity compared to WS9 (8% vs 0%), more of WS1 was unburned compared to WS9 (48% vs 2%). Additionally, a greater proportion of WS9 burned at low and moderate severity (98%) compared to WS1

TABLE 1 Holiday Farm Fire burn metrics (a) including soil burn severity (i) and basal area mortality (ii), and watershed characteristics (b) for WS1 and WS9.

	WS1	WS9
a) Holiday Farm Fire burn metrics		
(i) Soil Burn Severity (%)		
Unburned	48	2
Low severity	42	88
Moderate severity	1	10
High severity	8	0
(ii) Basal area		
Unburned	70	36
Low severity (1%–25%)	9	18
Moderate severity (25%–75%)	12	33
High severity (>75%)	2	11
b) Watershed characteristics		
Drainage area (ha)	96	8.5
Elevation range (m)	439–1027	426–731
Mean aspect (degrees)	286	211
Stand age (years)	~50	~500
Pre-fire land-use history	Logged, burned	Undisturbed
Slope (%)	60	60

(43%), and basal area mortality was higher at WS9 across all severities (Table 1) (Stratton, 2021).

2.1.2 | Experimental Watersheds 1 and 9

WS1 and WS9 are both lower-elevation experimental watersheds within the HJA (Figure 1). Elevation is slightly higher at WS1, and both watersheds have similarly steep slopes of roughly 60% (Table 1). The geology of both watersheds is highly weathered Oligocene tuffs and breccias that are prone to mass wasting. Soils are loamy, have high infiltration capacity, and are well-drained in most locations (Dyrness, 1969; Dyrness & Hawk, 1972; Rothacher, 1970). The largest differences between watersheds are in their drainage area (96 ha for WS1 and 8.5 ha for WS9), pre-fire forest age, and land-use history (Table 1). The forest in WS1 is approximately 50 years old, as it was 100% clearcut between 1962 and 1966, and then burned following logging in 1967. Pre-fire overstory vegetation consisted of planted Douglas-fir (*Pseudotsuga menziesii* (Mirbel); Dyrness, 1973) with occasional red alder (*Alnus rubra* Bong.), bigleaf maple (*Acer macrophyllum* Pursh.), and western hemlock (*Tsuga heterophylla*) (Halpern & Lutz, 2013). The understory consisted of vine maple (*Acer circinatum* Pursh.), red huckleberry (*Vaccinium parvifolium* Sm.), and sword fern (*Polystichum munitum*). WS9 was a designated as a reference watershed, leaving it relatively undisturbed with forest overstory age of approximately 500 years. Pre-fire vegetation was dominated by old-growth Douglas-fir with an understory of emergent Douglas-fir, western hemlock, Pacific yew (*Taxus brevifolia*), and bigleaf maple (Hawk, 1978).

2.2 | Available data

The HJA has numerous long-term datasets including hydrometric and biogeochemical data. We retrieved continuous stream discharge (HF004; Johnson, Harpold, et al., 2023) and stream chemistry data (CF002; Johnson & Fredriksen, 2019a) for WS1 and WS9 (Figure 1). Discharge at the gage stations was calculated as an average of 5-minute intervals from stage height (HF004; Johnson et al., 2021). At HJA, routine stream water samples are collected proportionally to streamflow (Fredriksen, 1969). Samples are composited over 1-week intervals at the gages, and three 1-week samples are composited in the lab before analysis at Cooperative Chemical Analytical Laboratory at Oregon State University (CCAL, Oregon State University, Corvallis, OR). Data on concentrations and fluxes are provided as three-week averages and are referred to as proportional samples from hereon (Johnson & Fredriksen, 2019a). Rainfall totals and precipitation chemistry (CP002; Johnson & Fredriksen, 2019b) were retrieved from the nearest weather station (PRIMET) (Figure 1). Precipitation totals for each collection period were calculated over the same time intervals as proportional stream chemistry (Johnson & Fredriksen, 2019a; Johnson & Fredriksen, 2019b). Additional details on calculations of

stream discharge, sample collection and lab analyses for chemistry are available in the metadata and summarized by Johnson et al. (2021).

2.3 | Event stream sample collection and analysis

After the September 2020 fire, instantaneous stream water samples were collected during the first four rain events to quantify stream chemistry. These events occurred in September, October, November and December 2020, hereon referred to as event samples. Event samples were collected at 8-hour intervals using ISCO automatic samplers (Teledyne ISCO, Lincoln, NE, USA) installed at WS1 and WS9 stream gage stations. Sampling started before each rain event and continued until streamflow was similar to pre-event levels. Unlike proportional stream samples collected routinely at HJA, samples collected during rain events represented an instantaneous measurement of stream chemical concentrations. Each 400 mL sample was filtered through a pre-ashed Whatman GF/F filter (pore size 0.7 µm), and frozen immediately after filtering. All stream sample analyses were conducted by CCAL, the same laboratory as the long-term water chemistry. Analytical methods and detection limits for all analyses are described on the CCAL web page (<https://ccal.oregonstate.edu/>). Here we focus on dissolved organic carbon (DOC), nitrate (NO_3^-), magnesium (Mg^{2+}), calcium (Ca^{2+}), sulfate (SO_4^{2-}), chloride (Cl^-), potassium (K^+), and phosphate (PO_4^{3-}). Units for all analytes are measured in mg L^{-1} except for NO_3^- (mg N/L), PO_4^{3-} (mg P/L), DOC (mg C/L) and SO_4^{2-} (mg S/L) (CF007; Johnson, 2024). From hereon we present all analytes in mg L^{-1} for simplicity.

2.4 | Analytical methods

2.4.1 | Hydrometric characterization

To characterize overall catchment wetness before and after the Holiday Farm Fire, we analysed precipitation totals for each year within our data record (Table S1). Specifically, we compared mean annual rainfall totals and mean fall rainfall totals recorded before (2003–2019) and after (2021–2023) the Holiday Farm Fire. We defined the fall season as September 1 through December 31 for each year of record. We limited our study to this timeframe as it corresponded with (1) roughly the onset and wet-up of the rainy season in PNW wet forests, and (2) the timing of our four rain events occurring immediately following the Holiday Farm Fire in 2020. To further characterize differences in catchment wetness and to identify potential drivers of constituent mobilization from the landscape to the stream, we calculated peak hourly rainfall intensities for each rain event (Murphy et al., 2015). Precipitation data from PRIMET were used for both WS1 and WS9. We focused our analysis on fall and annual rainfall inputs to the system given little snowpack develops at the lower elevation sites at HJA (Bierlmaler & McKee, 1989; Johnson et al., 2021; Jones & Perkins, 2010).

To evaluate post-fire differences in streamflow, we examined (1) total annual flows, (2) fall mean daily flows and (3) fall low flows pre- and post-fire. Fall low flow discharge was calculated using the 5th percentile flow discharge (referred to as baseflow) recorded between 1 September and 31 December of each year (Table S1). To effectively compare stream response between WS1 and WS9, which are different in drainage area, discharge values recorded at each stream gage were divided by corresponding catchment area and reported in mm hr^{-1} . Streamflow response immediately following the fire (September – December 2020) was only interpreted through the lens of immediate post-fire shifts in infiltration dynamics, given recharge dynamics for the majority of the year were under pre-fire conditions and shifts in evapotranspiration loss due to vegetation mortality would likely be minimal in this short period.

2.4.2 | Comparison of pre- and post-fire proportional stream chemistry

To compare differences in stream response between WS1 and WS9 following the Holiday Farm Fire, we limited our study years to those where proportional stream chemistry data were available at both sites (2003–2021) and fall months of each year (September–December). Pre-fire stream chemistry sample sizes were much larger ($n = 95/96$ for WS1/WS9), than post-fire samples ($n = 11/12$ for WS1/WS9). To determine if there were statistical differences between the pre- and post-fire stream solutes, we bootstrapped the data 3000 times, sub-sampling using a sample size of 10. The resultant distribution of Wilcoxon rank sum tests p -values was compared, and differences were evaluated for median p -values at alpha <0.1 .

2.4.3 | Evaluating post-fire shifts in streamflow contributions during rain events using principal component analysis and end-member mixing analysis

To assess potential post-fire shifts in flow path activation during rain events following the Holiday Farm Fire, stream chemistry collected during rain events at WS1 and WS9 were used in principal component analysis (PCA) and end-member mixing analysis (EMMA) following the methods of Christophersen and Hooper (1992). Due to a lack of hill-slope chemistry data specific to WS1 and WS9, we retrieved major ion chemistry collected from soil lysimeters in Watershed 10 (WS10) (HF024; McGuire, 2020) as a proxy for shallow preferential flow paths from each watershed to the stream. WS10 is located within the lower elevations of HJA and has similar geology, soils, and precipitation inputs as WS1 and WS9. As a proxy for groundwater contributions to streamflow, we retrieved major ion chemistry from a non-riparian well in WS1 (well D7, CF011; Wondzell & Corson-Rikert, 2016). Data were collected during baseflow conditions (Wondzell & Corson-Rikert, 2016). We used precipitation chemistry from PRIMET rainfall collector. EMMA was completed for the rain events in September and October at both watersheds. Tracer selections and end-member mixing scenarios were based on criteria adapted from Christophersen and

Hooper (1992). Tracers of Mg^{2+} , Ca^{2+} , Cl^- , NO_3^- , SO_4^{2-} and K^+ were included in PCA. Data were centered and scaled to achieve normal distribution and PCA was run using the R package PCAtools (Blighe & Lun, 2022). To determine the relative proportions of stream runoff derived from retained end-members, hydrograph separations were completed for each rain event at each site. In some cases, stream observations happened to lie outside the mixing domain defined by the selected end-members, resulting in negative fractions of relative contributions. In this case, negative fractions were forced to zero and other contributions were assumed to be a mixture of the remaining end-members only (Bush et al., 2023; Liu et al., 2004).

2.4.4 | Characterizing rain event concentration-discharge behaviour

While PCA and EMMA allowed us to estimate overall source contributions to the stream across each individual rain event, we used C-Q hysteresis analysis to compare differences in the timing of source water contributions between WS1 and WS9. Concentration was related to time series of discharge to visualize C-Q loops during individual rain events occurring from September through December. C-Q dynamics were evaluated for DOC , NO_3^- and PO_4^{3-} which represent primarily shallow, biologically active (or biogenic) sources to streamflow, and Mg^{2+} , K^+ , Ca^{2+} and SO_4^{2-} , which represent primarily bedrock-derived (or geogenic) sources (Herndon et al., 2015; Johnson et al., 2024; Li et al., 2021; Murphy et al., 2018; Sullivan et al., 2019; Zhi et al., 2019). We classified C-Q loops based on their clockwise or anticlockwise relationship with discharge.

3 | RESULTS

3.1 | Hydrologic response following fire

Hydrograph response during the period of study reflected the timing of Mediterranean rainfall and snow melt patterns at WS1 and WS9 (Figure S1). In many years, daily mean streamflow begins to increase in late-September or October. During the post-fire years of record (2021–2023) mean daily discharge values were within the range of the daily mean and standard deviation values calculated for the pre-fire years (2003–2019) (Figure 2, Table S1, Figure S1).

In the 16 years preceding the fire, mean annual precipitation total was 2131 mm and mean fall precipitation total was 941 mm (Table S1). Mean annual stream discharge totals were higher at WS1 than at WS9 (Table S1). Mean fall flows were lower and fall baseflows were higher at WS1 (Table 2, Figure 2).

In the 3 years following the fire, mean annual precipitation totals, mean fall precipitation totals, and annual stream discharge totals decreased slightly compared to pre-fire years (Table S1). Mean fall flows declined at WS1 and increased at WS9. Baseflows during fall slightly increased at both watersheds, and this was more pronounced at WS9 (Table 2, Figure 2).

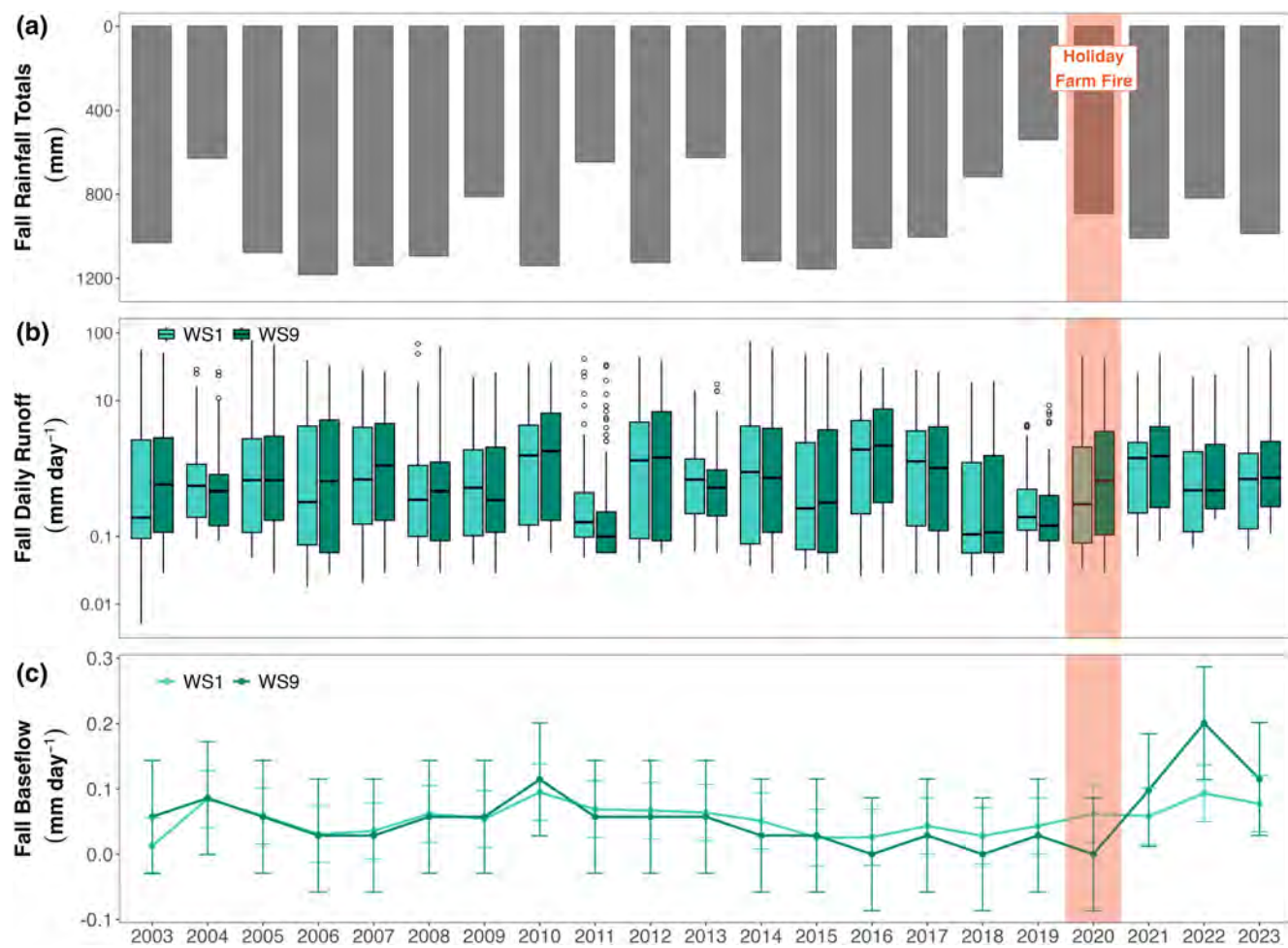


FIGURE 2 Fall rainfall totals (mm) for each year of study (a). Fall mean daily runoff (mm day^{-1}) for each year of study (b). For each boxplot the lower and upper hinges correspond to the first and third quartiles (the 25th and 75th percentiles). Upper and lower whiskers extend from the hinge to the smallest and largest values no further than 1.5 times the interquartile range. Data beyond the end of the whiskers are considered outliers. Fall baseflow (Q5 for September – December) runoff for each year of study (c). Error bars indicate measurement uncertainty for low flows (± 0.043 for WS1 and ± 0.086 for WS9) (HF004; Johnson et al., 2024).

TABLE 2 Mean streamflow metrics for fall flow and fall baseflow at WS1 and WS9. Mean values are calculated for each metric during pre-fire (2003–2019) and post-fire years (2021–2023). Standard deviations are given in parentheses. Fall and annual precipitation and streamflow totals for each year are given in Table S1.

Site	Variable	Units	Pre-fire	Post-fire
WS1	Mean fall flow	mm day^{-1}	2.58 (6.01)	2.45 (5.54)
	Mean fall baseflow	mm day^{-1}	0.05 (0.02)	0.08 (0.02)
WS9	Mean fall flow	mm day^{-1}	2.86 (6.11)	3.28 (6.49)
	Mean fall baseflow	mm day^{-1}	0.04 (0.03)	0.14 (0.05)

3.2 | Post-fire stream chemistry

Proportional stream constituent concentrations for our selected solutes increased following the Holiday Farm Fire at both WS1 and WS9, except for DOC (Figure 3). We observed the largest increases in pre- and post-fire concentrations for NO_3^- , PO_4^{3-} , and SO_4^{2-} at both sites, in addition to K^+ at WS9 ($p < 0.1$). Though not significant, we observed post-fire increases in Mg^{2+} , Ca^{2+} and Cl^- concentrations at both watersheds and K^+ at WS1.

3.3 | Rain event response

Rainfall totals increased from 4 mm during the September rain event to 229 mm in the December event (Table 3). Peak rainfall intensity increased with each subsequent rain event until December. Rain event durations increased through time with the exception of the November event, which was the shortest event. Streamflow and stream chemical responses to rain events of increasing magnitude differed between WS1 and WS9 (Figure 4, Figure 5, Table S2). Runoff

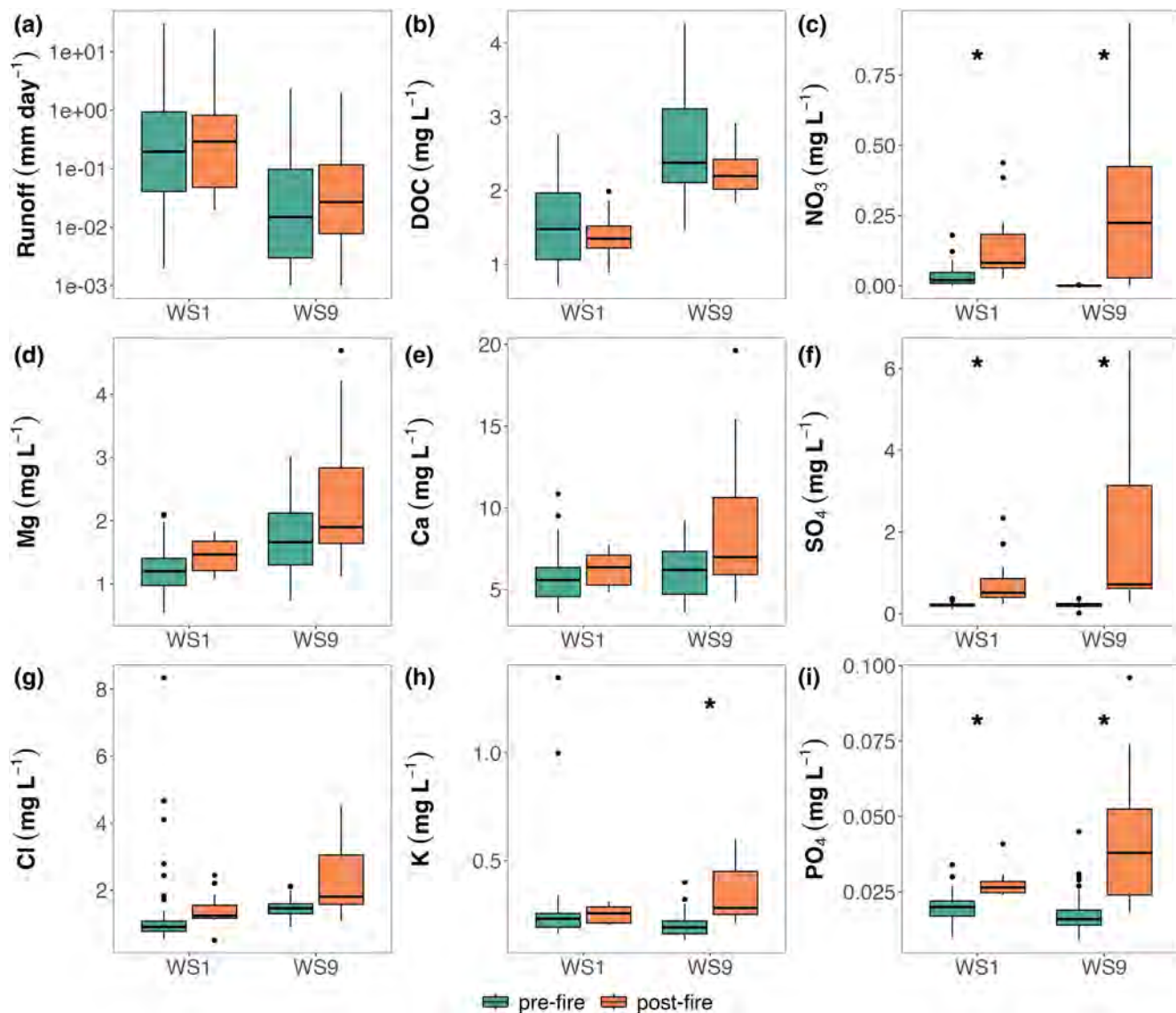


FIGURE 3 Pre- and post-fire comparisons of fall runoff (mm hr^{-1}) (a) and fall proportional stream chemistry for: Dissolved organic carbon (b), nitrate (c), magnesium (d), calcium (e), sulfate (f), chloride (g), potassium (h) and phosphate (i). WS1: Pre-fire $n = 95$, post-fire $n = 12$. WS9: Pre-fire $n = 96$, post-fire $n = 11$. For each boxplot the lower and upper hinges correspond to the first and third quartiles (the 25th and 75th percentiles). Upper and lower whiskers extend from the hinge to the smallest and largest values no further than 1.5 times the interquartile range. Data beyond the end of the whiskers are considered outliers. Asterisks indicate significance level results of bootstrapped Wilcoxon Rank Sum Test, where * indicates $p < 0.1$. Note units for: NO_3^- (mg N/L), PO_4^{3-} (mg P/L), DOC (mg C/L) and SO_4^{2-} (mg S/L) as stated in the methods.

TABLE 3 Rainfall total (mm), peak rainfall intensity (mm hr^{-1}), and rainfall duration (rounded to the nearest hour) measured for rain events between September and December 2020.

	September	October	November	December
Total (mm)	4	115	145	229
Peak intensity (mm hr^{-1})	0.3	9.1	12.2	6.6
Duration (hours)	145	169	88	305

response was greater at WS9 for all but the December event (Figure 4). Concentrations of all solutes except for K^+ at both sites and PO_4^{3-} at WS1 increased from the September to October events and decreased from October to November and November to December events (Figure 5, Table S2). We observed the largest increase in NO_3^- during the October rain event at both sites, with

NO_3^- values increasing from 0.03 mg L^{-1} to 0.19 mg L^{-1} at WS1 and from 0.01 mg L^{-1} to 0.17 mg L^{-1} at WS9. At WS1, PO_4^{3-} mean values remained relatively constant throughout all rain events (Table S2). Concentrations of K^+ were similar during September and October rain events and declined during the November and December rain events at both sites (Figure 5, Table S2).

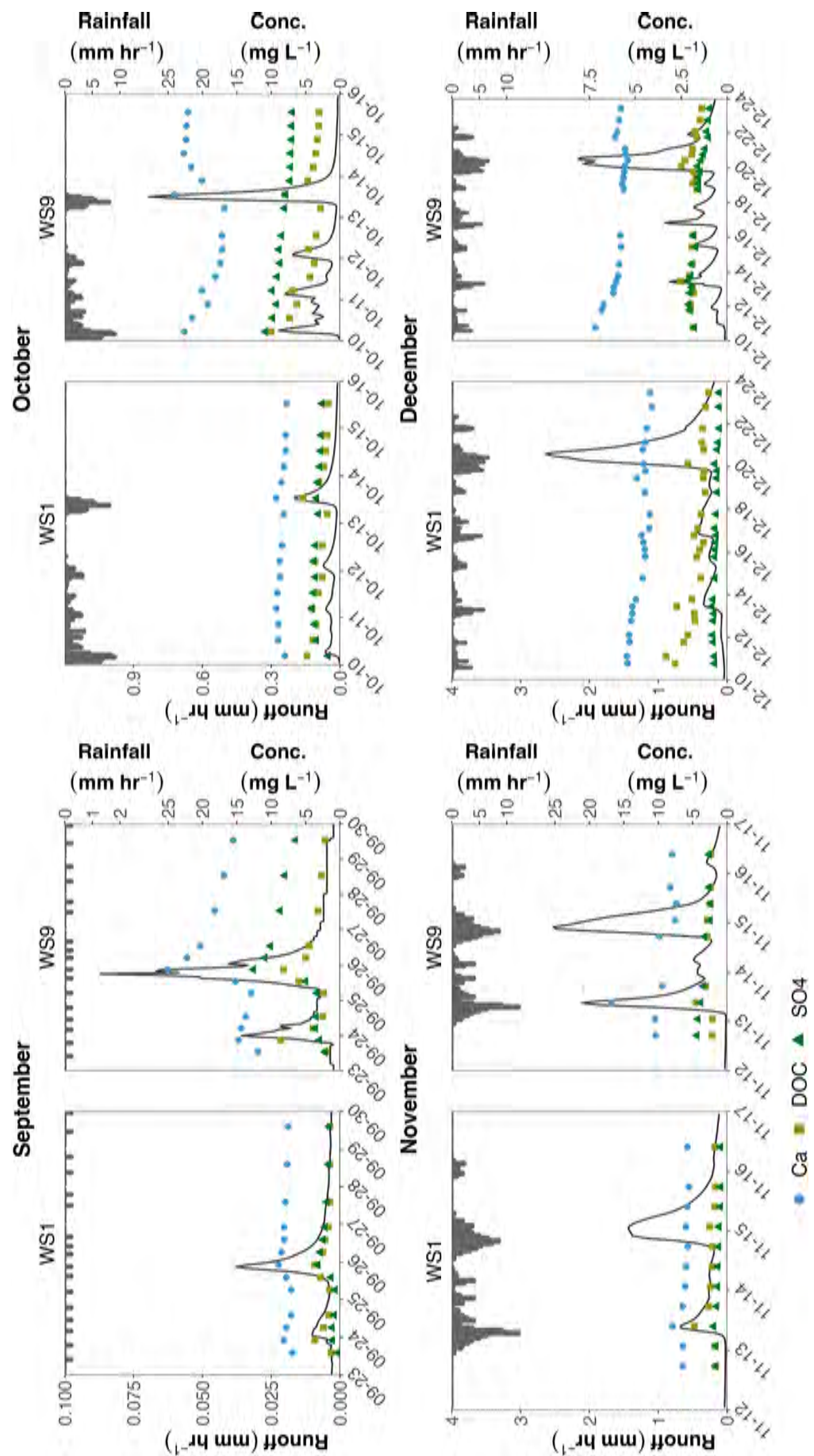


FIGURE 4 Time-series of hourly PRIMET precipitation totals (mm hr^{-1}), mean hourly runoff (mm hr^{-1}), and stream chemistry sample concentrations (Conc., mg L^{-1}) collected approximately every 8-hours during post-fire rain events in September, October, November and December 2020 for Watershed 1 (WS1) and Watershed 9 (WS9). Note units for DOC (mg C/L) and SO_4^{2-} (mg S/L) as stated in the methods. Time-series for additional constituents are given in Figure S2 of the supporting information. Rainfall totals, peak intensities, and rain event durations are given in Table 3.

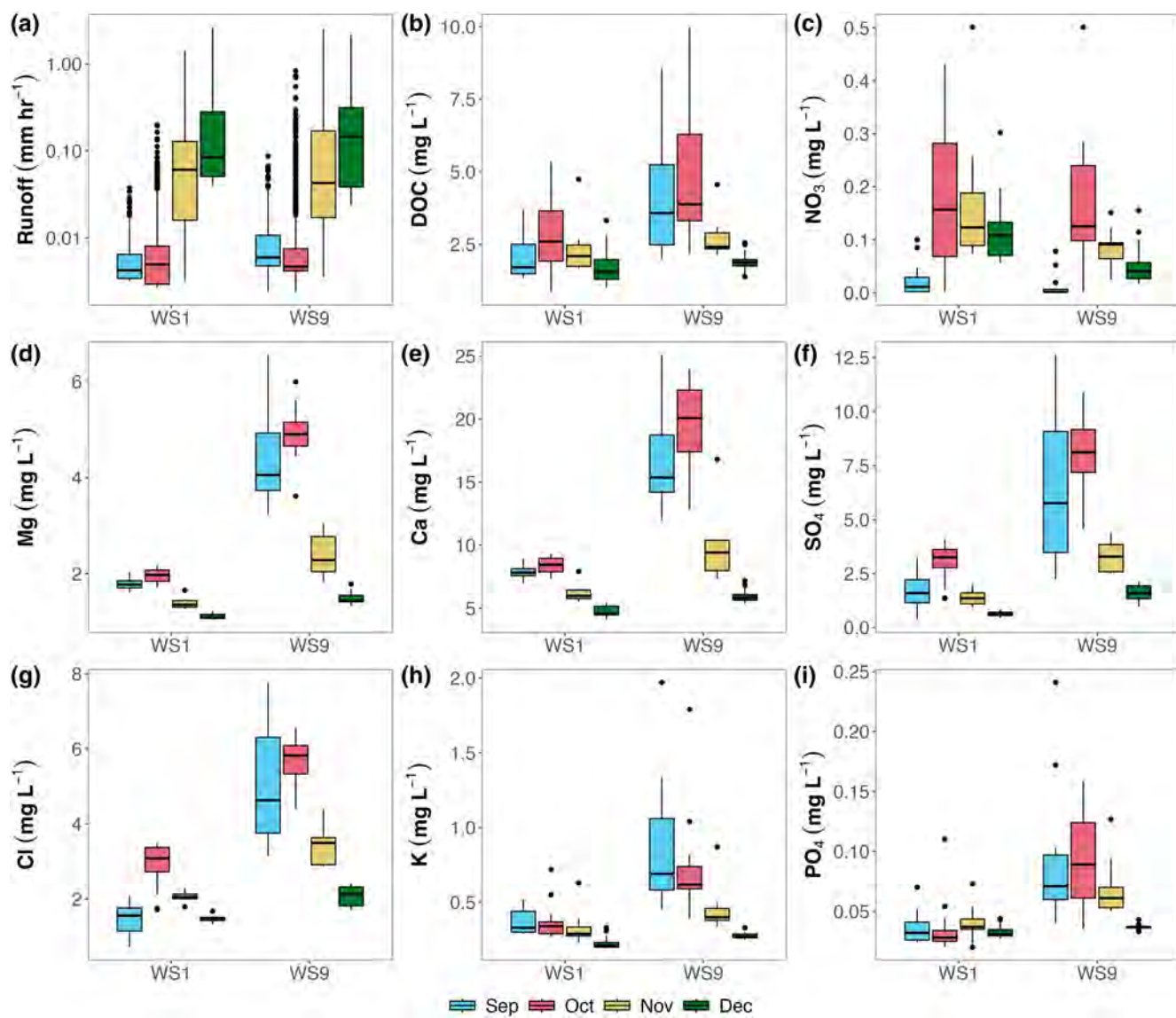


FIGURE 5 Post-fire runoff (mm hr^{-1}) (a) and event stream chemistry samples for: Dissolved organic carbon (b), nitrate (c), magnesium (d), calcium (e), sulfate (f), chloride (g), potassium (h) and phosphate (i) collected from each site. For each boxplot the lower and upper hinges correspond to the first and third quartiles (the 25th and 75th percentiles). Upper and lower whiskers extend from the hinge to the smallest and largest values no further than 1.5 times the interquartile range. Data beyond the end of the whiskers are considered outliers. Note units for NO_3^- (mg N/L), PO_4^{3-} (mg P/L), DOC (mg C/L) and SO_4^{2-} (mg S/L) as stated in the methods.

3.3.1 | Principal component analysis and end-member mixing analysis

PCA was performed for the stream water geochemical dataset associated with each rain event at WS1 and WS9 (Figure 6). Both scenarios required three end-member mixing. The percent variance explained by the first two principal components (PC1 and PC2) for WS1 was 84% and 76% for WS9. When projected into principal component space, stream samples exhibited distinct clustering corresponding to each rain event. End-members of soil water, groundwater, and rainwater chemistry approximately triangulate the stream sample clusters, with September and October rain event samples clustering between the rainfall and soil water end-members, and November and

December rain event samples clustering between rainfall and groundwater end-members at both sites.

Relative contributions of each end-member shifted with rain events of increasing magnitude and hydrologic connectivity, and differed between WS1 and WS9 (Figure 6, Table S3). WS1 exhibited relatively consistent contributions to streamflow across rain events: with the exception of the October event, all storms had highest contributions from rain, followed by groundwater and soil water. Streamflow contributions were more dynamic across rain events at WS9 compared to WS1, particularly with respect to soil water contributions, which decreased with each rain event (Figure 6d). At both sites, relative contributions of rainfall to streamflow were highest during the November and December rain events.

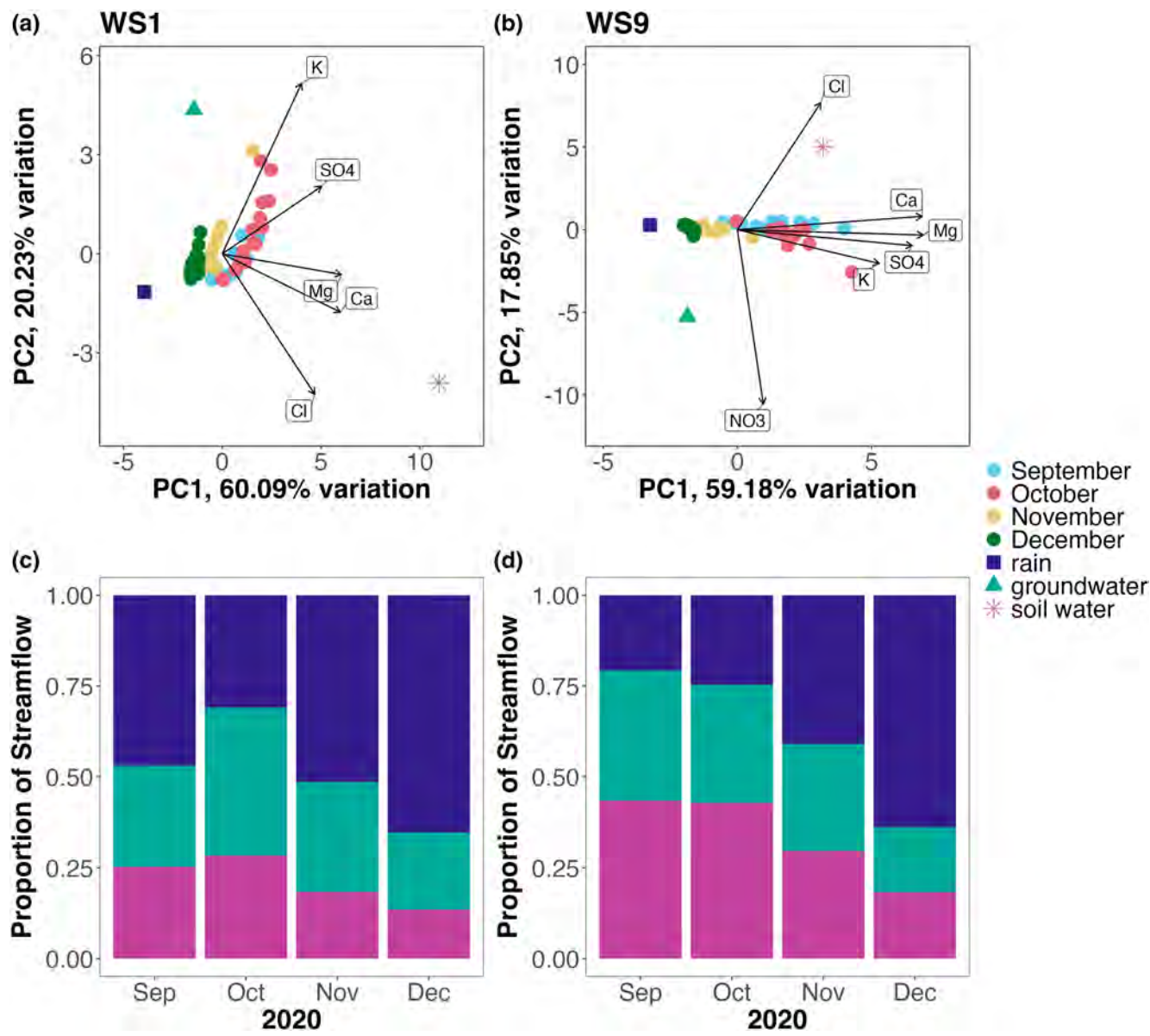


FIGURE 6 Two-dimensional principal component analysis (PCA) results for each rain event (circles) occurring at WS1 (a) and WS9 (b), and relative contributions of rain (squares), groundwater (triangles) and soil water to streamflow during each rain event at WS1 (c) and WS9 (d) calculated in end-member mixing analysis (EMMA).

3.3.2 | Concentration-discharge response

C-Q behaviours differed between WS1 and WS9 for biogenic solutes during the initial rain events (September and October) that had the lowest rainfall totals, but generally exhibited similar behaviours during the late fall higher rainfall total events (November and December) (Figure 7, Figure S3, Figure 8). In WS1, biogenic solutes exhibited clockwise C-Q behaviour across all events with the exception of PO_4^{3-} during the December event (Figure 8, Figure S2). In WS9, biogenic C-Q behaviour was more variable during the September and October events (Figure 8, Figure S2). In September,

DOC C-Q was clockwise during the first pulse of the hydrograph, then anticlockwise during the second pulse of the hydrograph, while NO_3^- was anticlockwise, and PO_4^{3-} was clockwise (Figures 7 and 8, Figure S3). During the October rain event, DOC was anticlockwise, NO_3^- was clockwise, and PO_4^{3-} was clockwise/ anticlockwise. During the November and December events, DOC was anticlockwise/ clockwise, while NO_3^- and PO_4^{3-} were clockwise. Geogenic solutes exhibited more similar behaviour across rain events and between sites compared to biogenic solutes with the exception of Ca^{2+} and Mg^{2+} during the October event, and Cl^- during the December rain event (Figure 8, Figure S3).

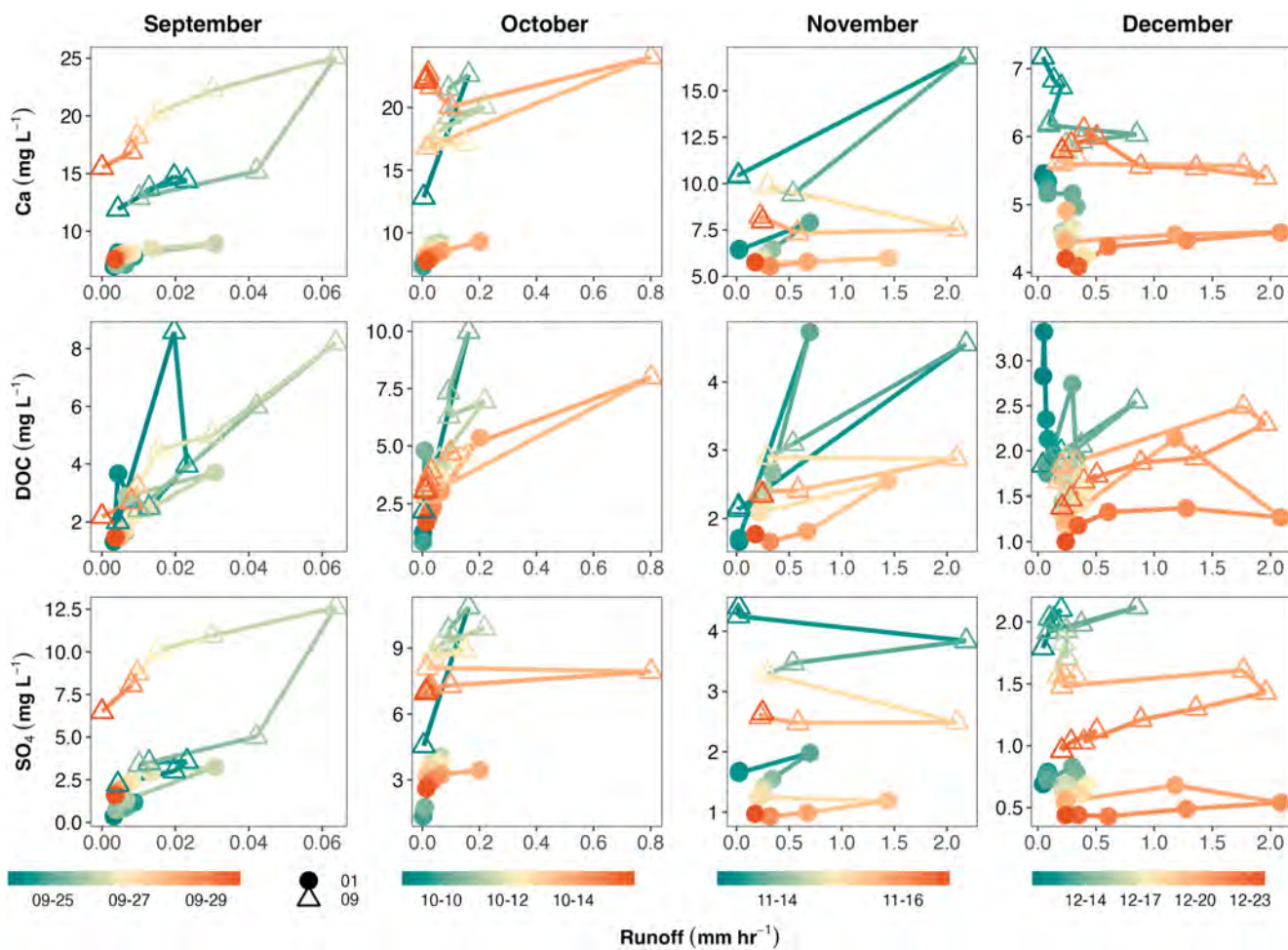


FIGURE 7 Concentration-discharge (C-Q) hysteresis loops for calcium, dissolved organic carbon, and sulfate collected during September through December 2020 rain events in WS1 (filled circles) and WS9 (open triangles). C-Q plots for additional solutes are given in Figure S3. Summary classifications for C-Q behaviour can be found in Figure 8.

4 | DISCUSSION

Understanding hydrological and biogeochemical responses to wildfire is often hindered by the lack of pre-fire data. Following the 2020 Holiday Farm Fire in Oregon, we evaluated a rare trove of pre- and post-fire water chemistry and hydrologic data and conducted rain event sampling in two watersheds that experienced low and low-moderate burn severity within the HJ Andrews (HJA) Experimental Forest. Although the watersheds had only a small proportion of high severity burn, we observed significant increases in fall post-fire concentrations of NO_3^- , PO_4^{3-} and SO_4^{2-} compared to pre-fire, but did not see significant changes in DOC or other analytes. However, hydrologic differences do not explain post-fire increases in stream chemistry, as fall mean streamflow, annual total streamflow, and annual precipitation totals were similar in pre-fire and post-fire years. Event sampling revealed that the greatest increases in concentrations occurred during the first two rain events following the fire, despite having low rainfall totals. Using EMMA and C-Q analysis of rain event samples, we draw attention to likely shifts in hydrologic flow paths and resulting changes in stream water chemistry with increasing hydrologic

connectivity during fall wet-up between watersheds with differing burn severity.

4.1 | Fire increased some streamflow metrics and altered stream water chemistry, but response varied likely due to differences in fire severity

Post-fire baseflows were higher at the more severely burned watershed (Figure 2), but stream water chemistry response was similar between watersheds (Figure 3). Increased streamflow immediately following wildfire is well documented in prior studies, which have shown the greatest increases in hydrologic impacts during the first several years post-fire (Ebel & Mirus, 2014; Niemeyer et al., 2020; Noske et al., 2016; Vieira et al., 2016). Burn severity and percent area burned have been positively correlated with increased annual flows, peak flows, and low flows (Feikema et al., 2013; Hallema et al., 2017; Kinoshita et al., 2014; Saxe et al., 2018; Wampler et al., 2023). The elevated fall baseflows (low flows) combined with the lack of increase in annual or fall flows in WS9 may signal that low-moderate burn

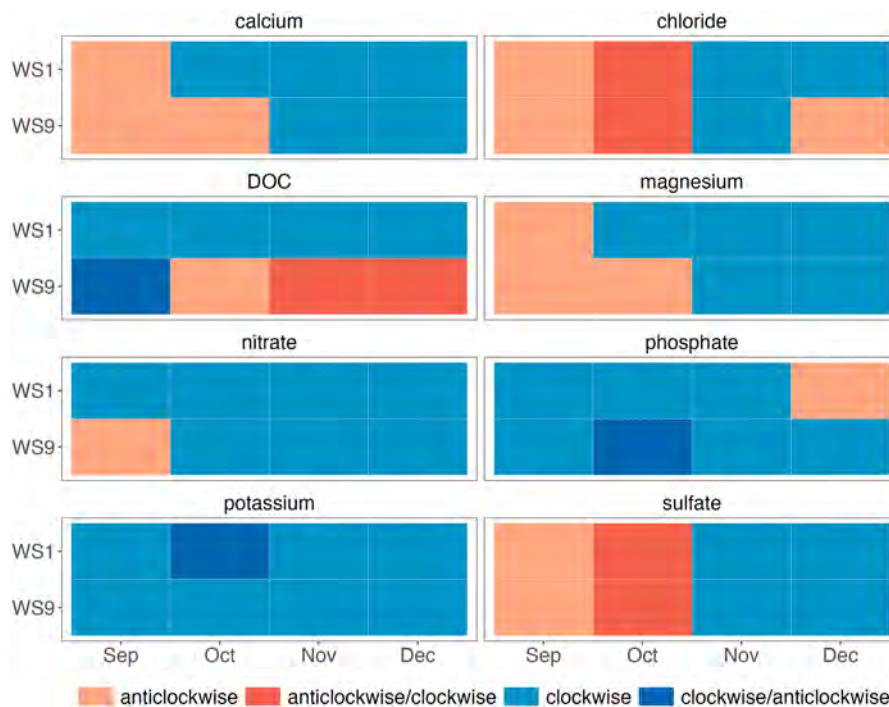


FIGURE 8 Summary of concentration-discharge (C-Q) hysteretic behaviour of primarily biogenic (DOC, nitrate, phosphate) and primarily geogenic (magnesium, potassium, calcium, sulfate, chloride) constituents for each rain event in each watershed. Clockwise behaviour is indicated by blue boxes, anticlockwise by orange boxes. In instances where different C-Q behaviour was observed between rainfall pulses within an event, solutes that initially exhibited anticlockwise behaviour are shown in dark orange and those that were initially clockwise are shown in dark blue. C-Q plots for solutes are given in Figure 7 and Figure S3.

severity had slightly greater hydrologic effect than the low severity burn, but only during the lowest of low flows. While these lowest flows would not propagate to have a meaningful impact on mean fall or total annual streamflow within the timeframe of our study, increases in baseflow can have both negative (e.g., habitat loss) and positive (e.g., short term increases in water yield) implications for ecosystem health and water sustainability.

Similar to other post-fire studies, we observed increases in post-fire stream chemistry for the majority of biogenic and geogenic solute concentrations of proportional samples (Figure 3). While we interpret proportional samples through the lens of differing constituent concentrations, samples may also be interpreted in terms of flux because they were collected compositionally, and therefore represent exports from each watershed (Johnson & Fredriksen, 2019a). Increases in stream solute concentrations post-fire have been linked to the export of pyrogenic materials from hillslopes to streams in fire impacted systems (Myers-Pigg et al., 2017; Roebuck Jr. et al., 2018; Wagner et al., 2015), which are additionally mobilized by precipitation inputs to the system (Bellé et al., 2021; Masiello & Berhe, 2020; Moody & Martin, 2001). Post-fire stream concentrations of biogenically derived constituents like nitrogen are complex and are largely impacted by altered soil moisture, hydrologic flowpaths, soil temperature, and soil microbial populations following wildfire (Koyama et al., 2010, 2012; Meixner et al., 2006). However, nitrogen and phosphorous have generally been shown to increase in streams post-fire (Chanasyk et al., 2003; Rhoades et al., 2019; Rust et al., 2018; Sherson et al., 2015; Smith et al., 2011). In the absence of fire, biogenically derived constituents have been shown to increase during the first rain events after a summer dry period or drought (Hood et al., 2006; Mosley, 2015), and this may play a role in the heightened concentrations of biogenic solutes during the September and October rain

events (Figure 5). Prior studies show that cations generally follow nutrient trends, increasing post-fire as a function of burned area and burn severity (Bitner et al., 2001; Rust et al., 2018; Smith et al., 2011) and at HJA we measured post-fire increases in Ca^{2+} , Mg^{2+} and K^+ . Variability in cation concentrations that we observed between watersheds could be attributed to differential subsurface flow paths associated with soil hydrophobicity and decreased infiltration or related to more moderate burn severity in WS9 relative to WS1. Stream SO_4^{2-} and Cl^- increased in both watersheds, consistent with the studies synthesized in Paul et al. (2022). Elevated SO_4^{2-} concentrations have also been observed in temperate environments due to increased delivery of ash to streams following the burning of organic matter (Bêche et al., 2005).

Decreases in DOC are less commonly observed post-fire. In a synthesis of post-fire stream responses, Paul et al. (2022) found only 26% of studies observed decreases in DOC and these were generally associated with high fire temperatures ($\geq 450^\circ\text{C}$). Lower post-fire DOC concentrations following high severity fires have been reported by other studies (Rodríguez-Cardona et al., 2020; Roebuck Jr et al., 2022; Santos et al., 2019). One explanation for lower DOC could be the loss and transformation of surface soils to charred materials following wildfire, leaving a less soluble store of organic carbon available for export to streams post-fire (Bostick et al., 2021; Hohner et al., 2016; Santín et al., 2016). However, some studies have found increases in DOC following low severity fires (Santos et al., 2019). Overall, fire processes are complex and highly spatially and temporally variable depending on fire severity, time since fire, and the location of fire relative to the stream (Rust et al., 2019). Thus, further study would be warranted to compare and quantify stream DOC concentrations in relation to availability of DOC in surface soils, specifically following low-to-moderate and mixed severity wildfires.

4.2 | Rainfall magnitude resulted in increased streamflow but a variable response in stream chemistry

In Mediterranean climates, the first rain event frequently results in high stream concentrations of solutes (Hood et al., 2006; Tague et al., 2008). In the wet forests of the PNW, precipitation inputs after a dry period shift streamflow source from deeper groundwater to shallow subsurface flow pathways, resulting in flushing of solutes to streams (Hood et al., 2006; Tague et al., 2008). Post-fire at HJA, multiple solute concentrations were notably higher during the September and October events compared to the November and December events, despite having relatively low rainfall totals and peak rainfall intensities (Figure 5, Table 3). Solute flushing has been measured in other systems where rainfall inputs increase hydrologic connectivity from various source areas following a prolonged dry period, similar to the dry summers we observe at the HJ Andrews (Burns et al., 2016; Johnson et al., 2023; Rademacher et al., 2005). However, wildfires can disrupt flow paths through the destruction of the surface and shallow subsurface organic layers, inhibiting infiltration and leading to elevated surface runoff in streams immediately following fire (Cerdà & Robichaud, 2009). Interestingly, during the later fall events in November and December, concentrations of primarily geogenically derived solutes (Ca^{2+} , Mg^{2+} , K^+ and SO_4^{2-}) declined, which suggests that the diluting effects from increased hydrologic connectivity outweighed the impacts of fire on solute concentrations. Though we measured the highest rainfall intensity during the November event, stream chemistry response was relatively dampened compared to that during the September and October events (Figure 5). Therefore, regardless of rainfall intensity, in times of high catchment moisture and hydrologic connectivity, rainfall entering the system would have reduced contact with soil water and groundwater and would be more chemically similar to rainfall. These findings are supported by work at HJA where high transit times of precipitation to streams were measured (McGuire & McDonnell, 2010; Segura, 2021). Differences in streamflow sources indicate shifts in flow path activation and connection to the stream with increased wetting as suggested by end-member mixing analysis and concentration-discharge dynamics.

4.3 | Flow paths differed with increasing rainfall magnitude and between watersheds with differing burn severity

Our EMMA and C-Q hysteresis evaluation identified distinct differences in post-fire rain event responses between WS1 and WS9 (Figures 6–8, Figure S2). Prior studies have shown that wildfire can alter runoff processes, causing shifts in subsurface flow, and impacting the quantity and quality of water delivered from uplands to streams (Ebel et al., 2012; Moody & Ebel, 2012). We noted stark contrast in streamflow contributions from groundwater and soil water between study watersheds, with soil water contributing proportionally more to

streamflow at WS9 compared to WS1. This could be due to the rapid mobilization and transport of solutes from the soil surface and shallow subsurface resulting from reduced canopy cover and increased hydrophobicity of the soil immediately following the Holiday Farm Fire, which was more pronounced at WS9. Additionally, we observed a more dynamic response to rainfall inputs at WS9, with the proportion of streamflow exhibiting a higher degree of variability among end-members and across each rain event.

Prior studies in unburned watersheds have observed that during rain events, biogenic solutes often exhibit clockwise C-Q behaviour and attributed this to mobilization or flushing of instream or riparian solutes on the rising limb of the hydrograph (Hood et al., 2006; McGlynn & McDonnell, 2003). Yet, our C-Q analysis showed differences in responses between WS1 and WS9, particularly for biogenic solutes. Although clockwise hysteresis behaviour was observed consistently in WS1 for DOC , NO_3^- and PO_4^{3-} , WS9 did not display consistent hysteretic behaviour across any of the rain events for DOC , and only during late fall events for NO_3^- , and PO_4^{3-} . This inconsistency in biogenic C-Q responses between catchments could be related to geologic influences on shallow flow paths and wet-up behaviour, and disturbances within the shallow subsurface and riparian zone following the Holiday Farm Fire. Burning may have disrupted near-stream processes or altered the degree of heterogeneity in biogenic sources (Bodí et al., 2014; Murphy et al., 2018; Roebuck Jr et al., 2022) resulting in differing hysteretic behaviour. In contrast to biogenic solutes, geogenic solutes generally exhibited the same C-Q behaviours in WS1 and WS9, implying the deeper subsurface flow paths were similar or not largely altered following fire. The higher concentrations of Mg^{2+} , K^+ and Ca^{2+} in WS9 could be related to rates of wet up of the soil profile and subsequent impacts to hydrologic flow paths or that the burning of organic matter released these ions (Bêche et al., 2005).

4.4 | Future directions and constraints for understanding wildfire impacts to streamflow

Current understanding of stream chemistry response to fire primarily come from studies of high severity fires (e.g., Mast & Clow, 2008; Murphy & Writer, 2011; Rhoades et al., 2019) in landscapes that did not have pre-fire data (e.g., Murphy et al., 2012; Rust et al., 2018; Santos et al., 2019). Additionally, although stream nutrient dynamics have been studied following fire, less is known about the long-term impacts of wildfire on other stream solutes, and particularly so for low and moderate severity fires (Bixby et al., 2015). Our study leveraged a rare long-term pre-fire dataset paired with rapid-response post-fire rain event sampling with the goal of better understanding the role of hydrologic connectivity in post-fire water quality. Results of our study highlight future needs for wildfire research, particularly following low and low-to-moderate severity wildfire.

Prior wildfire research has identified the need to understand long-term dynamics, particularly for streamflow and nutrient delivery

to streams (Murphy et al., 2018; Roebuck Jr et al., 2022). Several studies have found immediate increases in streamflow followed by declines 10+ years after wildfire (Murphy et al., 2018; Niemeyer et al., 2020). Our data set extends through 2023, only 3 years following the Holiday Farm Fire, highlighting the need for continued monitoring specifically in WS1 and WS9. Fortunately, continued streamflow measurements and stream water chemistry are planned at HJA. In addition, targeted post-fire monitoring including long-term vegetation plots and sediment traps will contribute to increased understanding of catchment scale post-fire impacts, both within the context of the Holiday Farm Fire and the mixed severity Lookout Fire that burned 68% of HJA in 2023.

There are additional datasets that we suggest would improve understanding of the legacy of low-moderate severity wildfire at HJA. For example, collecting and analysing water isotopes (Birch et al., 2021; Segura et al., 2019), radon (Johnson et al., 2024; Smerdon & Gardner, 2022), or age tracers (e.g., CFCs or SF₆; Warix et al., 2023) in conjunction with stream chemistry would allow for comparison of water age and chemistry across flow paths to support inferences in rates and timing of hydrologic connectivity to the stream. Additionally, post-fire soil sampling and soil extractions would allow for both a more accurate characterization of post-fire soil chemistry, and composition which would allow us to disentangle physical and chemical inferences from shallow subsurface flow paths from hill-slopes to streams. Lastly, the use of LiDAR imaging to quantify landscape scale vegetation recovery would allow future wildfire researchers to better understand long-term shifts in land-cover, particularly following low-moderate severity fire where less is known.

Although the HJA databases provided extensive information pre-fire, we acknowledge that our findings in this study are constrained by the available data. First, the long-term chemistry data extends across the pre- and post-fire years, and this proportional sampling was designed to quantify multiweek averages and seasonal to annual fluxes, but not instantaneous concentrations. We did not have consistent high frequency event-based samples from the pre-fire period for these watersheds. Another challenge stemmed from the limited hill-slope chemistry available for PCA and EMMA. While we were able to select soil water and groundwater chemistry data collected during the fall wet-up in pre-fire years, we did not have on site representation of these end-member data post-fire. Although groundwater data were collected from WS1, the lack of groundwater data available specific to WS9 was evident in the apparent missing end-member in our PCA analysis (Figure 6). However, end-member chemistry data used in our study are representative of generally similar soils and geologies between watersheds, and are applied broadly to make inferences about relative shifts in flow paths following fire. Finally, while slopes, soils, and underlying geology are similar between the two burned watersheds, forest age, land-use history, and drainage area differ greatly (Table 1). Such factors are likely to influence runoff efficiency and the hydrologic flow paths from the landscape to the stream (Birch et al., 2021; Bush et al., 2020; Zema et al., 2021) but given that we did not have additional measurements (e.g., pre- and post-fire canopy interception) these factors cannot be normalized.

5 | CONCLUSIONS

In our study, we explored immediate stream chemistry responses to mixed severity forest fires and built on long-term pre-fire data. Specifically, our results indicate notable differences in stream chemical responses in watersheds with differing burn severity during rain events immediately following the September 2020 Holiday Farm Fire, and as rain events contributed to increasingly more saturated conditions through December. Solute concentrations, concentration-discharge behaviour, and end-member mixing analysis revealed altered hydrologic and biogeochemical dynamics between pre- and post-fire, with a greater difference observed in the low-moderately burned watershed. Total annual flows and mean flows remained fairly consistent post-fire, while the lowest fall baseflows showed small increases in the low-moderately burned watershed. Stream water concentrations of nitrate, phosphate and sulfate significantly increased following fire. During post-fire rain events, streamflow contributions and C-Q behaviour of biogenic solute concentrations were more dynamic at the low-moderate severity burned watershed. Differences in stream chemical response were especially pronounced during the September and October rain events when hydrologic connectivity was lowest. We suggest these increases were related to greater streamflow inputs from soil water and groundwater in the low-moderately burned watershed compared to the low severity burned watershed. Our findings highlight the value of prioritizing stream and watershed sampling to disentangle differences in timing of source contributions to post-fire streamflow and stream chemistry. This will be of particular interest following the Lookout Fire, a mixed severity fire that burned 68% of HJA during late Summer 2023. Such findings are critical to predicting responses to mixed severity fires across the Pacific Northwest and the western United States especially where forested watersheds provide drinking water for downstream communities.

ACKNOWLEDGEMENTS

This material is based upon work supported by the National Science Foundation NSF EAR-2034232 (Sidney A. Bush, Pamela L. Sullivan), NSF EAR-2012796 (Pamela L. Sullivan). Data were provided by the HJ Andrews Experimental Forest research program, funded by NSF Long Term Ecological Research DEB-2025755, US Forest Service Pacific Northwest Research Station, and Oregon State University. We thank Kelly Christiansen for the creation of the site map displayed in Figure 1 and Greg Downing for field collection of long-term hydrology and chemistry data, and for conducting rain event sampling.

DATA AVAILABILITY STATEMENT

The data are cited in the methods with full citations in the references.

ORCID

Sidney A. Bush  <https://orcid.org/0000-0002-8359-7927>
Sherri L. Johnson  <https://orcid.org/0000-0002-4223-3465>
Kevin D. Bladon  <https://orcid.org/0000-0002-4182-6883>
Pamela L. Sullivan  <https://orcid.org/0000-0001-8780-8501>

REFERENCES

Agbeshie, A. A., Abugre, S., Atta-Darkwa, T., & Awuah, R. (2022). A review of the effects of forest fire on soil properties. *Journal of Forestry Research*, 33, 1419–1441. <https://doi.org/10.1007/s11676-022-01475-4>

Ávila, A., Piñol, J., Rodà, F., & Neal, C. (1992). Storm solute behaviour in a montane mediterranean forested catchment. *Journal of Hydrology*, 140(1–4), 143–161. [https://doi.org/10.1016/0022-1694\(92\)90238-Q](https://doi.org/10.1016/0022-1694(92)90238-Q)

Balfour, V. N., Doerr, S. H., & Robichaud, P. R. (2014). The temporal evolution of wildfire ash and implications for post-fire infiltration. *International Journal of Wildland Fire*, 23(5), 733–745. <https://doi.org/10.1071/WF13159>

Bart, R. (2016). A regional estimate of postfire streamflow change in California. *Water Resources Research*, 52(2), 1465–1478. <https://doi.org/10.1002/2014WR016553>

Bêche, L. A., Stephens, S. L., & Resh, V. H. (2005). Effects of prescribed fire on a Sierra Nevada (California, USA) stream and its riparian zone. *Forest Ecology and Management*, 218(1–3), 37–59. <https://doi.org/10.1016/j.foreco.2005.06.010>

Bellè, S. L., Berhe, A. A., Hagedorn, F., Santin, C., Schiedung, M., van Meerveld, I., & Abiven, S. (2021). Key drivers of pyrogenic carbon redistribution during a simulated rainfall event. *Biogeosciences*, 18(3), 1105–1126. <https://doi.org/10.5194/bg-18-1105-2021>

Bernal, S., von Schiller, D., Sabater, F., & Martí, E. (2013). Hydrological extremes modulate nutrient dynamics in mediterranean climate streams across different spatial scales. *Hydrobiologia*, 719, 31–42. <https://doi.org/10.1007/s10750-012-1246-2>

Bierlmaier, F. A., & McKee, A. (1989). Climatic summaries and documentation for the primary meteorological station, HJ Andrews Experimental Forest, 1972 To 1984.(No. PNW-GTR-242). US Department of Agriculture, Forest Service, Pacific Northwest Research Station. [10.2737/PNW-GTR-242](https://doi.org/10.2737/PNW-GTR-242)

Bieroza, M. Z., & Heathwaite, A. L. (2015). Seasonal variation in phosphorus concentration–discharge hysteresis inferred from high-frequency in situ monitoring. *Journal of Hydrology*, 524, 333–347. <https://doi.org/10.1016/j.jhydrol.2015.02.036>

Birch, A. L., Stallard, R. F., & Barnard, H. R. (2021). Precipitation characteristics and land cover control wet season runoff source and rainfall partitioning in three humid tropical catchments in Central Panama. *Water Resources Research*, 57(2), e2020WR028058. <https://doi.org/10.1016/j.jhydrol.2021.126138>

Bitner, K., Gallaher, B., & Mullen, K. (2001). Review of wildfire effects on chemical water quality (No. LA-13826-MS). Los Alamos National Lab. (LANL), Los Alamos, NM (United States). [10.2172/781455](https://doi.org/10.2172/781455)

Bixby, R. J., Cooper, S. D., Gresswell, R. E., Brown, L. E., Dahm, C. N., & Dwire, K. A. (2015). Fire effects on aquatic ecosystems: An assessment of the current state of the science. *Freshwater Science*, 34(4), 1340–1350. <https://doi.org/10.1086/684073>

Bladon, K. D., Emelko, M. B., Silins, U., & Stone, M. (2014). Wildfire and the future of water supply. *Environmental Science & Technology*, 48(16), 8936–8943.

Blighe, K., & Lun, A. (2022). PCAtools: PCAtools: Everything principal components analysis. R Package Version 2.10. <https://github.com/kevinblighe/PCAtools>

Bodí, M. B., Martin, D. A., Balfour, V. N., Santín, C., Doerr, S. H., Pereira, P., Cerdà, A., & Mataix-Solera, J. (2014). Wildland fire ash: Production, composition and eco-hydro-geomorphic effects. *Earth-Science Reviews*, 130, 103–127. <https://doi.org/10.1016/j.earscirev.2013.12.007>

Bonada, N., & Resh, V. H. (2013). Mediterranean-climate streams and rivers: Geographically separated but ecologically comparable freshwater systems. *Hydrobiologia*, 719, 1–29. <https://doi.org/10.1007/s10750-013-1634-2>

Bostick, K. W., Zimmerman, A. R., Goranov, A. I., Mitra, S., Hatcher, P. G., & Wozniak, A. S. (2021). Biolability of fresh and photo-degraded pyrogenic dissolved organic matter from laboratory-prepared chars. *Journal of Geophysical Research Biogeosciences*, 126(5), e2020JG005981. <https://doi.org/10.1029/2020JG005981>

Bowes, M. J., Jarvie, H. P., Halliday, S. J., Skeffington, R. A., Wade, A. J., Loewenthal, M., ... Palmer-Felgate, E. J. (2015). Characterising phosphorus and nitrate inputs to a rural river using high-frequency concentration–flow relationships. *Science of the Total Environment*, 511, 608–620. <https://doi.org/10.1016/j.scitotenv.2014.12.086>

Burns, M. A., Barnard, H. R., Gabor, R. S., McKnight, D. M., & Brooks, P. D. (2016). Dissolved organic matter transport reflects hillslope to stream connectivity during snowmelt in a montane catchment. *Water Resources Research*, 52(6), 4905–4923. <https://doi.org/10.1002/2015WR017878>

Bush, S. A., Birch, A. L., Warix, S. R., Sullivan, P. L., Gooseff, M. N., McKnight, D. M., & Barnard, H. R. (2023). Dominant source areas shift seasonally from longitudinal to lateral contributions in a montane headwater stream. *Journal of Hydrology*, 617(129), 134. <https://doi.org/10.1016/j.jhydrol.2023.129134>

Bush, S. A., Stallard, R. F., Ebel, B. A., & Barnard, H. R. (2020). Assessing plot-scale impacts of land use on overland flow generation in Central Panama. *Hydrological Processes*, 34(25), 5043–5069. <https://doi.org/10.1002/hyp.13924>

Butturini, A., Alvarez, M., Bernal, S., Vazquez, E., & Sabater, F. (2008). Diversity and temporal sequences of forms of DOC and NO₃-discharge responses in an intermittent stream: Predictable or random succession? *Journal of Geophysical Research Biogeosciences*, 113(G3). <https://doi.org/10.1029/2008JG000721>

Butturini, A., Gallart, F., Latron, J., Vazquez, E., & Sabater, F. (2006). Cross-site comparison of variability of DOC and nitrate c–q hysteresis during the autumn–winter period in three Mediterranean headwater streams: A synthetic approach. *Biogeochemistry*, 77, 327–349. <https://doi.org/10.1007/s10533-005-0711-7>

Cerdà, A., & Robichaud, P. R. (2009). Fire effects on soil infiltration. In *Fire effects on soils and restoration strategies* (pp. 97–120). CRC Press.

Chanasylk, D. S., Whitson, I. R., Mapfumo, E., Burke, J. M., & Prepas, E. E. (2003). The impacts of forest harvest and wildfire on soils and hydrology in temperate forests: A baseline to develop hypotheses for the boreal plain. *Journal of Environmental Engineering and Science*, 2, S51–S62. <https://doi.org/10.1139/s03-034>

Christophersen, N., & Hooper, R. P. (1992). Multivariate analysis of stream water chemical data the use of principal components analysis for the end-member mixing problem. *Water Resources Research*, 28, 99–107. <https://doi.org/10.1029/91WR02518>

D'Odorico, P., & Rigon, R. (2003). Hillslope and channel contributions to the hydrologic response. *Water Resources Research*, 39(5). <https://doi.org/10.1029/2002WR001708>

Doerr, S. H., Shakesby, R. A., & Walsh, R. (2000). Soil water repellency: Its causes, characteristics and hydro-geomorphological significance. *Earth-Science Reviews*, 51(1–4), 33–65. [https://doi.org/10.1016/S0012-8252\(00\)00011-8](https://doi.org/10.1016/S0012-8252(00)00011-8)

Dyrness, C. T. (1969). Hydrologic properties of soils on three small watersheds in the western cascades of Oregon. U.S. Forest Service Research Paper, PNW-111, Pacific Northwest Forest and Range Experiment Station, Portland, OR.

Dyrness, C. T. (1973). Early stages of plant succession following logging and burning in the western cascades of Oregon. *Ecology*, 54(1), 57–69. <https://doi.org/10.2307/1934374>

Dyrness, C. T., & Hawk, G. (1972). Vegetation and soils of the Hi-15 watersheds, H.J. Andrews experimental forest. <https://andrewsforest.oregonstate.edu/pubs/pdf/pub1742.pdf>

Ebel, B. A., & Mirus, B. B. (2014). Disturbance hydrology: Challenges and opportunities. *Hydrological Processes*, 28(19), 5140–5148. <https://doi.org/10.1002/hyp.10256>

Ebel, B. A., & Moody, J. A. (2017). Synthesis of soil-hydraulic properties and infiltration timescales in wildfire-affected soils. *Hydrological Processes*, 31(2), 324–340. <https://doi.org/10.1002/hyp.10998>

Ebel, B. A., Moody, J. A., & Martin, D. A. (2012). Hydrologic conditions controlling runoff generation immediately after wildfire. *Water Resources Research*, 48(3). <https://doi.org/10.1029/2011WR011470>

Emelko, M. B., Stone, M., Silins, U., Allin, D., Collins, A. L., Williams, C. H. S., Martens, A. M., & Bladon, K. D. (2016). Sediment-phosphorus dynamics can shift aquatic ecology and cause downstream legacy effects after wildfire in large river systems. *Global Change Biology*, 22(3), 1168–1184. <https://doi.org/10.1111/gcb.13073>

Evans, C., & Davies, T. D. (1998). Causes of concentration/discharge hysteresis and its potential as a tool for analysis of episode hydrochemistry. *Water Resources Research*, 34(1), 129–137. <https://doi.org/10.1029/97WR01881>

Feikema, P. M., Sherwin, C. B., & Lane, P. N. (2013). Influence of climate, fire severity and forest mortality on predictions of long term streamflow: Potential effect of the 2009 wildfire on Melbourne's water supply catchments. *Journal of Hydrology*, 488, 1–16. <https://doi.org/10.1016/j.jhydrol.2013.02.001>

Fredriksen, R. L. (1969). A battery powered proportional stream water sampler. *Water Resources Research*, 5(6), 1410–1413.

Gellis, A. C. (2013). Factors influencing storm-generated suspended-sediment concentrations and loads in four basins of contrasting land use, humid-tropical Puerto Rico. *Catena*, 104, 39–57. <https://doi.org/10.1016/j.catena.2012.10.018>

Godsey, S. E., Kirchner, J. W., & Clow, D. W. (2009). Concentration–discharge relationships reflect chemostatic characteristics of US catchments. *Hydrological Processes: An International Journal*, 23(13), 1844–1864. <https://doi.org/10.1002/hyp.7315>

Guarch-Ribot, A., & Butturini, A. (2016). Hydrological conditions regulate dissolved organic matter quality in an intermittent headwater stream. From drought to storm analysis. *Science of the Total Environment*, 571, 1358–1369. <https://doi.org/10.1016/j.scitotenv.2016.07.060>

Hallema, D. W., Sun, G., Bladon, K. D., Norman, S. P., Caldwell, P. V., Liu, Y., & McNulty, S. G. (2017). Regional patterns of postwildfire streamflow response in the Western United States: The importance of scale-specific connectivity. *Hydrological Processes*, 31(14), 2582–2598. <https://doi.org/10.1002/hyp.11208>

Halpern, C. B., & Lutz, J. A. (2013). Canopy closure exerts weak controls on understory dynamics: A 30-year study of overstory–understory interactions. *Ecological Monographs*, 83(2), 221–237. <https://doi.org/10.1890/12-1696.1>

Hawk, G. M. (1978). HJ Andrews experimental forest reference stand system: Establishment and use history.

Herndon, E. M., Dere, A. L., Sullivan, P. L., Norris, D., Reynolds, B., & Brantley, S. L. (2015). Landscape heterogeneity drives contrasting concentration–discharge relationships in shale headwater catchments. *Hydrology and Earth System Sciences*, 19, 3333–3347. <https://doi.org/10.5194/hess-19-3333-2015>

Hohner, A. K., Cawley, K., Oropesa, J., Summers, R. S., & Rosario-Ortiz, F. L. (2016). Drinking water treatment response following a Colorado wildfire. *Water Research*, 105, 187–198. <https://doi.org/10.1016/j.watres.2016.08.034>

Holden, Z. A., Swanson, A., Luce, C. H., Jolly, W. M., Maneta, M., Oyler, J. W., Warren, D. A., Parsons, R., & Affleck, D. (2018). Decreasing fire season precipitation increased recent western US forest wildfire activity. *Proceedings of the National Academy of Sciences*, 115(36), E8349–E8357. <https://doi.org/10.1073/pnas.1802316115>

Hood, E., Gooseff, M. N., & Johnson, S. L. (2006). Changes in the character of stream water dissolved organic carbon during flushing in three small watersheds, Oregon. *Journal of Geophysical Research*, 111(G1), G01007. <https://doi.org/10.1029/2005JG000082>

Hooper, R. P., & Shoemaker, C. A. (1986). A comparison of chemical and isotopic hydrograph separation. *Water Resources Research*, 22, 1444–1454. <https://doi.org/10.1029/WR022i010p01444>

Jencso, K. G., McGlynn, B. L., Gooseff, M. N., Wondzell, S. M., Bencala, K. E., & Marshall, L. A. (2009). Hydrologic connectivity between landscapes and streams: Transferring reach-and plot-scale understanding to the catchment scale. *Water Resources Research*, 45(4). <https://doi.org/10.1029/2008WR007225>

Johnson, K., Christensen, J., Gardner, W. P., Sprenger, M., Li, L., Williams, K. H., Carroll, R. W. H., Brown, N. T. W., Beutler, C., Newman, A., & Sullivan, P. L. (2024). Shifting groundwater fluxes in bedrock fractures: Evidence from stream water radon and water isotopes. *Journal of Hydrology*, 131, 202. <https://doi.org/10.1016/j.jhydrol.2024.131202>

Johnson, K., Harpold, A., Carroll, R. W., Barnard, H., Raleigh, M. S., Segura, C., Li, L., Williams, K. H., Dong, W., & Sullivan, P. L. (2023). Leveraging groundwater dynamics to improve predictions of summer low-flow discharges. *Water Resources Research*, 59(8), e2023WR035126. <https://doi.org/10.1029/2023WR035126>

Johnson, S. (2024). Stream chemistry concentrations during storms at HJ Andrews experimental Forest stream gages post fire. <https://doi.org/10.6073/pasta/809735b6ef217b7c4ab4426f7285401f>

Johnson, S., Wondzell, S., & Rothacher, J. (2023). Stream discharge in gaged watersheds at the HJ Andrews experimental Forest, 1949 to present. <https://doi.org/10.6073/pasta/0066d6b04e736af5f234d95d97ee84f3>

Johnson, S. L., & Fredriksen, R. L. (2019a). Stream chemistry concentrations and fluxes using proportional sampling in the Andrews experimental Forest, 1968 to present (CP002). *Environmental Data Initiative*. <https://doi.org/10.6073/pasta/bb935444378d112d9189556fd22a441d>

Johnson, S. L., & Fredriksen, R. L. (2019b). Precipitation chemistry concentrations and fluxes, HJ Andrews experimental Forest, 1969 to present (CP002). *Environmental Data Initiative*. <https://doi.org/10.6073/pasta/2cee34b1d3c0836888444f9033c1c1c8>

Johnson, S. L., Henshaw, D., Downing, G., Wondzell, S., Schulze, M., Kennedy, A., ... Jones, J. A. (2021). Long-term hydrology and aquatic biogeochemistry data from HJ Andrews experimental Forest, Cascade Mountains, Oregon. *Hydrological Processes*, 35(5), e14187. <https://doi.org/10.1002/hyp.14187>

Jones, J. A., & Perkins, R. M. (2010). Extreme flood sensitivity to snow and forest harvest, western cascades, Oregon, United States. *Water Resources Research*, 46(12). <https://doi.org/10.1029/2009WR008632>

Kiewiet, L., van Meerveld, I., Stähli, M., & Seibert, J. (2020). Do stream water solute concentrations reflect when connectivity occurs in a small, pre-alpine headwater catchment? *Hydrology and Earth System Sciences*, 24, 3381–3398. <https://doi.org/10.5194/hess-24-3381-2020>

Kinoshita, A. M., Hogue, T. S., & Napper, C. (2014). Evaluating pre-and post-fire peak discharge predictions across western US watersheds. *JAWRA Journal of the American Water Resources Association*, 50(6), 1540–1557. <https://doi.org/10.1111/jawr.12226>

Koyama, A., Kavanagh, K. L., & Stephan, K. (2010). Wildfire effects on soil gross nitrogen transformation rates in coniferous forests of central Idaho, USA. *Ecosystems*, 13(7), 1112–1126. <https://doi.org/10.1007/s10021-010-9377-7>

Koyama, A., Stephan, K., & Kavanagh, K. L. (2012). Fire effects on gross inorganic N transformation in riparian soils in coniferous forests of central Idaho, USA: Wildfires v. prescribed fires. *International Journal of Wildland Fire*, 21(1), 69–78. <https://doi.org/10.1071/WF10132>

Larson-Nash, S. S., Robichaud, P. R., Pierson, F. B., Moffet, C. A., Williams, C. J., Spaeth, K. E., Brown, R. E., & Lewis, S. A. (2018). Recovery of small-scale infiltration and erosion after wildfires. *Journal of Hydrology and Hydromechanics*, 66(3), 261–270. <https://doi.org/10.1515/johh-2017-0056>

Lavabre, J., Torres, D. S., & Cernessson, F. (1993). Changes in the hydrological response of a small mediterranean basin a year after a wildfire. *Journal of Hydrology*, 142(1–4), 273–299. [https://doi.org/10.1016/0022-1694\(93\)90014-Z](https://doi.org/10.1016/0022-1694(93)90014-Z)

Lawler, D. M., Petts, G. E., Foster, I. D., & Harper, S. (2006). Turbidity dynamics during spring storm events in an urban headwater river system: The upper tame, west midlands. UK. *Science of the Total Environment*, 360(1-3), 109–126. <https://doi.org/10.1016/j.scitotenv.2005.08.032>

Li, L., Sullivan, P. L., Benettin, P., Cirpka, O. A., Bishop, K., Brantley, S. L., Knapp, J. L. A., van Meerveld, I., Rinaldo, A., Seibert, J., Wen, H., & Kirchner, J. W. (2021). Toward catchment hydro-biogeochemical theories. *WIREs Water*, 8, e1495. <https://doi.org/10.1002/wat2.1495>

Liu, F. J., Williams, M. W., & Caine, N. (2004). Source waters and flow paths in an alpine catchment, Colorado front range, United States. *Water Resources Research*, 40, W09401. <https://doi.org/10.1029/2004WR003076>

Lloyd, C. E., Freer, J. E., Johnes, P. J., & Collins, A. L. (2016). Testing an improved index for analysing storm discharge-concentration hysteresis. *Hydrology and Earth System Sciences*, 20(2), 625–632. <https://doi.org/10.5194/hess-20-625-2016>

Masiello, C. A., & Berhe, A. A. (2020). First interactions with the hydrologic cycle determine pyrogenic carbon's fate in the earth system. *Earth Surface Processes and Landforms*, 45(10), 2394–2398. <https://doi.org/10.1002/esp.4925>

Mast, M. A., & Clow, D. W. (2008). Effects of 2003 wildfires on stream chemistry in glacier National Park. *Montana. Hydrological Processes: An International Journal*, 22(26), 5013–5023. <https://doi.org/10.1002/hyp.7121>

McGlynn, B. L., & McDonnell, J. J. (2003). Quantifying the relative contributions of riparian and hillslope zones to catchment runoff. *Water Resources Research*, 39(11). <https://doi.org/10.1029/2003WR002091>

McGuire, K. (2020). Oxygen-18 isotope ratios, chemistry, and tracers in storm water from WS10 hillslope experiment in the HJ Andrews Experimental Forest, 2001–2003. <https://doi.org/10.6073/pasta/4fb341bdce5d020b7c18612335cc20c>

McGuire, K. J., & McDonnell, J. J. (2010). Hydrological connectivity of hillslopes and streams: Characteristic time scales and nonlinearities. *Water Resources Research*, 46(10). <https://doi.org/10.1029/2010WR009341>

McGuire, L. A., Rengers, F. K., Oakley, N., Kean, J. W., Staley, D. M., Tang, H., de Orla-Barile, M., & Youberg, A. M. (2021). Time since burning and rainfall characteristics impact post-fire debris-flow initiation and magnitude. *Environmental & Engineering Geoscience*, 27(1), 43–56. <https://doi.org/10.2113/EEG-D-20-00029>

Meixner, T., Fenn, M. E., Wohlgemuth, P., Oxford, M., & Riggan, P. (2006). N saturation symptoms in chaparral catchments are not reversed by prescribed fire. *Environmental Science and Technology*, 40(9), 2887–2894. <https://doi.org/10.1021/es051268z>

Moody, J. A., & Martin, D. A. (2001). Initial hydrologic and geomorphic response following a wildfire in the Colorado front range. *Earth Surface Processes and Landforms*, 26(10), 1049–1070. <https://doi.org/10.1002/esp.253>

Moody, J. A., & Ebel, B. A. (2012). Hyper-dry conditions provide new insights into the cause of extreme floods after wildfire. *Catena*, 93, 58–63. <https://doi.org/10.1016/j.catena.2012.01.006>

Mosley, L. M. (2015). Drought impacts on the water quality of freshwater systems; review and integration. *Earth-Science Reviews*, 140, 203–214.

Murphy, S. F., McCleskey, R. B., Martin, D. A., Writer, J. H., & Ebel, B. A. (2018). Fire, flood, and drought: Extreme climate events alter flow paths and stream chemistry. *Journal of Geophysical Research: Biogeosciences*, 123, 2513–2526. <https://doi.org/10.1029/2017JG004349>

Murphy, S. F., McCleskey, R. B., & Writer, J. H. (2012). *Effects of flow regime on stream turbidity and suspended solids after wildfire, Colorado front range* (Vol. 354, pp. 51–58). IAHS-AISH Publications.

Murphy, S. F., & Writer, J. H. (2011). Evaluating the effects of wildfire on stream processes in a Colorado front range watershed, USA. *Applied Geochemistry*, 26, S363–S364. <https://doi.org/10.1016/j.apgeochem.2011.03.061>

Murphy, S. F., Writer, J. H., McCleskey, R. B., & Martin, D. A. (2015). The role of precipitation type, intensity, and spatial distribution in source water quality after wildfire. *Environmental Research Letters*, 10(8), 084007.

Myers-Pigg, A. N., Louchouarn, P., & Teisserenc, R. (2017). Flux of dissolved and particulate low-temperature pyrogenic carbon from two high-latitude rivers across the spring freshet hydrograph. *Frontiers in Marine Science*, 4(38). <https://doi.org/10.3389/fmars.2017.00038>

Niemeyer, R. J., Bladon, K. D., & Woodsmith, R. D. (2020). Long-term hydrologic recovery after wildfire and post-fire forest management in the interior Pacific northwest. *Hydrological Processes*, 34(5), 1182–1197. <https://doi.org/10.1002/hyp.13665>

Nippgen, F., McGlynn, B. L., & Emanuel, R. E. (2015). The spatial and temporal evolution of contributing areas. *Water Resources Research*, 51(6), 4550–4573. <https://doi.org/10.1002/2014WR016719>

Nippgen, F., McGlynn, B. L., Marshall, L. A., & Emanuel, R. E. (2011). Landscape structure and climate influences on hydrologic response. *Water Resources Research*, 47(12). <https://doi.org/10.1029/2011WR011161>

Noske, P. J., Nyman, P., Lane, P. N., & Sheridan, G. J. (2016). Effects of aridity in controlling the magnitude of runoff and erosion after wildfire. *Water Resources Research*, 52(6), 4338–4357. <https://doi.org/10.1002/2015WR017611>

Nyman, P., Sheridan, G. J., Smith, H. G., & Lane, P. N. (2011). Evidence of debris flow occurrence after wildfire in upland catchments of south-east Australia. *Geomorphology*, 125(3), 383–401. <https://doi.org/10.1016/j.geomorph.2010.10.016>

Nyman, P., Sheridan, G. J., Smith, H. G., & Lane, P. N. (2014). Modeling the effects of surface storage, macropore flow and water repellency on infiltration after wildfire. *Journal of Hydrology*, 513, 301–313. <https://doi.org/10.1016/j.jhydrol.2014.02.044>

Paul, M. J., LeDuc, S. D., Lassiter, M. G., Moorhead, L. C., Noyes, P. D., & Leibowitz, S. G. (2022). Wildfire induces changes in receiving waters: A review with considerations for water quality management. *Water Resources Research*, 58(9), e2021WR030699. <https://doi.org/10.1029/2021WR030699>

Rademacher, L. K., Clark, J. F., Clow, D. W., & Hudson, G. B. (2005). Old groundwater influence on stream hydrochemistry and catchment response times in a small Sierra Nevada catchment: Sagehen Creek, California. *Water Resources Research*, 41, W02004. <https://doi.org/10.1029/2003WR002805>

Reilly, M. J., Zuspan, A., Halofsky, J. S., Raymond, C., McEvoy, A., Dye, A. W., Donato, D. C., Kim, J. B., Potter, B. E., Walker, N., Davis, R. J., Dunn, C. J., Bell, D. M., Gregory, M. J., Johnston, J. D., Harvey, B. J., Halofsky, J. E., & Kerns, B. K. (2022). Cascadia burning: The historic, but not historically unprecedented, 2020 wildfires in the Pacific northwest, USA. *Ecosphere*, 13(6), e4070. <https://doi.org/10.1002/ecs2.4070>

Rhoades, C. C., Chow, A. T., Covino, T. P., Fegel, T. S., Pierson, D. N., & Rhea, A. E. (2019). The legacy of a severe wildfire on stream nitrogen and carbon in headwater catchments. *Ecosystems*, 22, 643–657. <https://doi.org/10.1007/s10021-018-0293-6>

Rodríguez-Cardona, B. M., Coble, A. A., Wymore, A. S., Kolosov, R., Podgorski, D. C., Zito, P., Spencer, R. G. M., Prokushkin, A. S., & McDowell, W. H. (2020). Wildfires lead to decreased carbon and increased nitrogen concentrations in upland arctic streams. *Scientific Reports*, 10(1), 8722. <https://doi.org/10.1038/s41598-020-65520-0>

Roebuck, J. A., Jr., Bladon, K. D., Donahue, D., Graham, E. B., Grieber, S., Morgenstern, K., Norwood, M. J., Wampler, K. A., Erkert, L., Renteria, L., Danczak, R., Fricke, S., & Myers-Pigg, A. N. (2022). Spatio-temporal controls on the delivery of dissolved organic matter to streams following a wildfire. *Geophysical Research Letters*, 49(16), e2022GL099535. <https://doi.org/10.1029/2022GL099535>

Roebuck, J. A., Jr., Medeiros, P. M., Letourneau, M. L., & Jaffé, R. (2018). Hydrological controls on the seasonal variability of dissolved and particulate black carbon in the Altamaha river. *GA. Journal of Geophysical*

Research: *Biogeosciences*, 123(9), 3055–3071. <https://doi.org/10.1029/2018JG004406>

Rothacher, J. (1970). Increases in water yield following clear-cut logging in the Pacific northwest. *Water Resources Research*, 6(2), 653–658.

Rust, A. J., Hogue, T. S., Saxe, S., & McCray, J. (2018). Post-fire water-quality response in the western United States. *International Journal of Wildland Fire*, 27(3), 203–216. <https://doi.org/10.1071/WF17115>

Rust, A. J., Saxe, S., McCray, J., Rhoades, C. C., & Hogue, T. S. (2019). Evaluating the factors responsible for post-fire water quality response in forests of the western USA. *International Journal of Wildland Fire*, 28(10), 769–784. <https://doi.org/10.1071/WF18191>

Santín, C., Doerr, S. H., Kane, E. S., Masiello, C. A., Ohlson, M., de la Rosa, J. M., Preston, C. M., & Dittmar, T. (2016). Towards a global assessment of pyrogenic carbon from vegetation fires. *Global Change Biology*, 22(1), 76–91. <https://doi.org/10.1111/gcb.12985>

Santos, F., Wymore, A. S., Jackson, B. K., Sullivan, S. M. P., McDowell, W. H., & Berhe, A. A. (2019). Fire severity, time since fire, and site-level characteristics influence streamwater chemistry at baseflow conditions in catchments of the Sierra Nevada, California, USA. *Fire Ecology*, 15(1), 3. <https://doi.org/10.1186/s42408-018-0022-8>

Saxe, S., Hogue, T. S., & Hay, L. (2018). Characterization and evaluation of controls on post-fire streamflow response across western US watersheds. *Hydrology and Earth System Sciences*, 22(2), 1221–1237. <https://doi.org/10.5194/hess-22-1221-2018>

Segura, C. (2021). Snow drought reduces water transit times in headwater streams. *Hydrological Processes*, 35(12), e14437. <https://doi.org/10.1002/hyp.14437>

Segura, C., Noone, D., Warren, D., Jones, J. A., Tenny, J., & Ganio, L. M. (2019). Climate, landforms, and geology affect baseflow sources in a mountain catchment. *Water Resources Research*, 55(7), 5238–5254. <https://doi.org/10.1029/2018WR023551>

Sherson, L. R., Van Horn, D. J., Gomez-Velez, J. D., Crossey, L. J., & Dahm, C. N. (2015). Nutrient dynamics in an alpine headwater stream: Use of continuous water quality sensors to examine responses to wildfire and precipitation events. *Hydrological Processes*, 29(14), 3193–3207. <https://doi.org/10.1002/hyp.10426>

Sklash, M. G., & Farvolden, R. N. (1979). The role of groundwater in storm runoff. *Journal of Hydrology*, 43, 45–65. [https://doi.org/10.1016/0022-1694\(79\)90164-1](https://doi.org/10.1016/0022-1694(79)90164-1)

Smerdon, B. D., & Gardner, W. P. (2022). Characterizing groundwater flow paths in an undeveloped region through synoptic river sampling for environmental tracers. *Hydrological Processes*, 36(1), e14464. <https://doi.org/10.1002/hyp.14464>

Smith, H. G., Sheridan, G. J., Lane, P. N., Nyman, P., & Haydon, S. (2011). Wildfire effects on water quality in forest catchments: A review with implications for water supply. *Journal of Hydrology*, 396(1–2), 170–192. <https://doi.org/10.1016/j.jhydrol.2010.10.043>

Smith, T., Marshall, L., McGlynn, B., & Jencso, K. (2013). Using field data to inform and evaluate a new model of catchment hydrologic connectivity. *Water Resources Research*, 49(10), 6834–6846. <https://doi.org/10.1002/wrcr.20546>

Stratton, A. E. (2021). Pacific Northwest Regional Basal Area Mortality Calculations in Google Earth Engine - Unpublished Documentation (GEE_ba7_Metadata.docx). United States Department of Agriculture, Forest Service, Pacific Northwest Region, Data Resources Management.

Sullivan, P. L., Stops, M. W., Macpherson, G. L., Li, L., Hirmas, D. R., & Dodds, W. K. (2019). How landscape heterogeneity governs stream water concentration-discharge behavior in carbonate terrains (Konza prairie, USA). *Chemical Geology*, 527(118), 989. <https://doi.org/10.1016/j.chemgeo.2018.12.002>

Tague, C., Grant, G., Farrell, M., Choate, J., & Jefferson, A. (2008). Deep groundwater mediates streamflow response to climate warming in the Oregon cascades. *Climatic Change*, 86, 189–210. <https://doi.org/10.1007/s10584-007-9294-8>

Tetzlaff, D., Buttle, J., Carey, S. K., McGuire, K., Laudon, H., & Soulsby, C. (2015). Tracer-based assessment of flow paths, storage and runoff generation in northern catchments: A review. *Hydrological Processes*, 29(16), 3475–3490. <https://doi.org/10.1002/hyp.10412>

Uhlenbrook, S., Roser, S., & Tilch, N. (2004). Hydrological process representation at the meso-scale: The potential of a distributed, conceptual catchment model. *Journal of Hydrology*, 291(3–4), 278–296. <https://doi.org/10.1016/j.jhydrol.2003.12.038>

USDA Forest Service. (2020). Soil burn severity dataset for the holiday farm fire (OR4417212223120200908) occurring on the Willamette National Forest. National Forest Geospatial Technology and Applications Center, BAER Imagery Support Program, Salt Lake City, Utah, USA. <https://burnseverity.cr.usgs.gov/baer/baer-imagery-support-data-download>

Vieira, D. C. S., Malvar, M. C., Fernandez, C., Serpa, D., & Keizer, J. J. (2016). Annual runoff and erosion in a recently burn Mediterranean forest—the effects of plowing and time-since-fire. *Geomorphology*, 270, 172–183. <https://doi.org/10.1016/j.geomorph.2016.06.042>

Wagner, S., Cawley, K. M., Rosario-Ortiz, F. L., & Jaffé, R. (2015). In-stream sources and links between particulate and dissolved black carbon following a wildfire. *Biogeochemistry*, 124(1), 145–161. <https://doi.org/10.1007/s10533-015-0088-1>

Wampler, K. A., Bladon, K. D., & Faramarzi, M. (2023). Modeling wildfire effects on streamflow in the Cascade Mountains, Oregon, USA. *Journal of Hydrology*, 621(129), 585. <https://doi.org/10.1016/j.jhydrol.2023.129585>

Warix, S. R., Navarre-Sitchler, A., Manning, A. H., & Singha, K. (2023). Local topography and streambed hydraulic conductivity influence riparian groundwater age and groundwater-surface water connection. *Water Resources Research*, 59(9), e2023WR035044. <https://doi.org/10.1029/2023WR035044>

Westerling, A. L. (2016). Increasing western US forest wildfire activity: Sensitivity to changes in the timing of spring. *Philosophical Transactions of the Royal Society B: Biological Sciences*, 371(1696), 20150178. <https://doi.org/10.1098/rstb.2015.0178>

Wine, M. L., Cadol, D., & Makhnin, O. (2018). In ecoregions across western USA streamflow increases during post-wildfire recovery. *Environmental Research Letters*, 13(1), 014010. <https://doi.org/10.1088/1748-9326/aa9c5a>

Wondzell, S., & Corson-Rikert, H. (2016). Carbon dynamics in the hyporheic zone of a headwater mountain stream in the Cascade Mountains, Oregon – Watershed 1 at HJA – June 2013 to March 2014. <https://doi.org/10.6073/pasta/7a070aab134c1add4f239fab6318b4d7>

Zema, D. A., Plaza-Alvarez, P. A., Xu, X., Carra, B. G., & Lucas-Borja, M. E. (2021). Influence of forest stand age on soil water repellency and hydraulic conductivity in the mediterranean environment. *Science of the Total Environment*, 753(142), 6.

Zhi, W., Li, L., Dong, W., Brown, W., Kaye, J., Steefel, C., & Williams, K. H. (2019). Distinct source water chemistry shapes contrasting concentration-discharge patterns. *Water Resources Research*, 55(5), 4233–4251. <https://doi.org/10.1029/2018WR024257>

SUPPORTING INFORMATION

Additional supporting information can be found online in the Supporting Information section at the end of this article.

How to cite this article: Bush, S. A., Johnson, S. L., Bladon, K. D., & Sullivan, P. L. (2024). Stream chemical response is mediated by hydrologic connectivity and fire severity in a Pacific Northwest forest. *Hydrological Processes*, 38(7), e15231. <https://doi.org/10.1002/hyp.15231>